Optimized Theta Burst Stimulation with Extended Intervals Enhances Excitatory Inhibitory Balance

Morteza Salimi[1,2*], Milad Nazari[3,4,5], Jonathan Mishler[1,2,8], Jennifer Rodger[6,7] , Sahar Jomehpour[2], Jyoti Mishra[2,8] , Dhakshin S. Ramanathan[1,2,6,8,9*]

1- Research Service, VA San Diego Healthcare System, La Jolla, CA, 92161
2- NEATLabs, Department of Psychiatry, UC San Diego, La Jolla, CA, 92093
3- Department of Molecular Biology and Genetics, Aarhus University, Aarhus, Denmark
4- DANDRITE, The Danish Research Institute of Translational Neuroscience, Aarhus, Denmark
5- Center for Protein in Memory-PROMEMO, Danish National Research Foundation
6- Brain Plasticity, Perron Institute for Neurological and Translational Science, Nedlands, WA, Australia
7- School of Biological Sciences, University of Western Australia, Crawley, WA, Australia
8- Center of Excellence for Stress and Mental Health, VA San Diego Healthcare System, La Jolla, CA, 92161
9- Mental Health Care Line, VA San Diego Healthcare System, La Jolla, CA, 92161

*Corresponding Authors: Dhakshin S. Ramanathan, dramanathan@health.ucsd.edu; Morteza Salimi, msalimi@health.ucsd.edu

Graphical Abstract:

Varying inter-train intervals (ITIs) during theta burst stimulation (TBS) differentially modulates neuronal activity in the medial prefrontal cortex. Short ITIs (e.g., ITI 4 s) induce strong glutamatergic excitation but fail to induce long-term changes post-stimulation. By contrast, an extended ITI of 20 seconds (eTBS, green star) optimally enhances long-term excitability in glutamatergic neurons while suppressing GABAergic interneurons, indicating a shift in excitation-inhibition balance that promotes cortical plasticity.

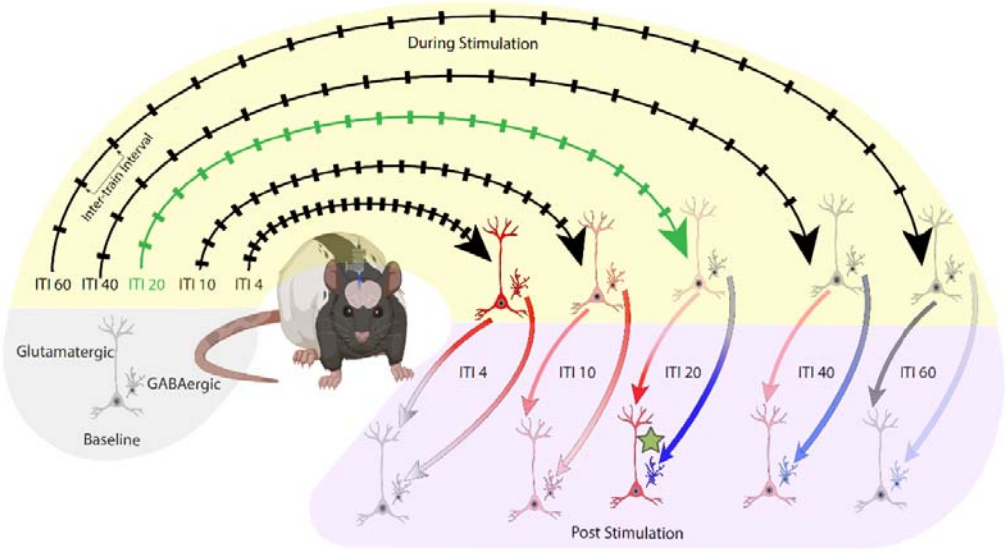

Summary

Electrical theta burst stimulation (TBS) with different inter-train intervals (ITIs) was first used to characterize bidirectional synaptic plasticity in brain slices. Despite a lack of understanding of mechanism, TBS has been adopted by rTMS research and clinical protocols to drive plasticity in the human brain, with variable results. To uncover how TBS modulates excitability *in vivo*, we systematically screen the impact of electrical TBS with different ITIs on rodent cortical neurons. Short inter-train intervals (4-10s) increased calcium activity in both glutamatergic and GABAergic neurons during stimulation, whereas extended ITIs (20s) yielded modest but significant activation of glutamatergic cells and minimal activation of GABAergic cells. TBS with an ITI of 20s emerged as a plasticity "sweet spot" that maximized long-term activation of glutamatergic neurons, potentially through suppression of GABAergic neurons(1–3). Translating our novel iTBS electrical stimulation protocol to rTMS interventions has the potential to deliver heightened plasticity and improved therapeutic outcomes.

Highlights

- Systematic manipulation of inter-train intervals (ITIs) reveals an optimal 20s ITI for TBS-induced plasticity.
- Extended ITIs enhance excitability in glutamatergic neurons while suppressing GABAergic activity.
- PV interneurons are preferentially recruited during short-interval TBS, limiting sustained plasticity.

Keywords: Theta burst stimulation; inter-train interval; glutamatergic neurons; GABAergic interneurons; calcium imaging; excitation-inhibition balance; single-cell analysis

Acknowledgements: Grant support includes: . The views expressed in this article are those of the authors and do not necessarily reflect the position or policy of the VA or the NIH. The funders had no role in the design of the study, data analysis, or decision to publish. The authors have no relevant biomedical conflicts of interest to disclose.

Introduction

Transcranial magnetic stimulation (TMS) was first demonstrated in 1985 by Tony Barker and colleagues, as a noninvasive method to stimulate the human cortex using brief magnetic pulses (4). In the ensuing decades, TMS stimulation protocols evolved to capitalize on patterned stimulation paradigms that mimic brain rhythms to induce synaptic plasticity (5,6). One major advance was the development of theta burst stimulation (TBS), delivering bursts of high-frequency pulses (typically 50 Hz triplets) repeated at a theta frequency (~5 Hz) (7). This patterned approach was inspired by seminal findings in hippocampal slices using electrical stimulation: that a series of high frequency bursts repeated at theta frequency intervals for 2 seconds was sufficient to produce long-term potentiation (LTP), likely by overcoming inhibitory gating (3,7,8). Huang et al. (2005) translating this concept to human TMS, found that multiple repeated TBS trains, spaced 8 seconds apart were required to produce long-lasting changes in cortical excitability (2). These foundational studies established repetitive TBS as a powerful tool for modulating excitability in vivo (9). TBS delivered using both electrical stimulation (in animals) and electromagnetic fields (in humans and animals) has since become important in both experimental and clinical contexts (1,5). Because it packs hundreds of pulses into a few minutes, TBS is believed to elicit longer-lasting potentiation or depression of cortical activity far more efficiently than conventional rTMS protocols (10), leading to widespread use both for probing cortical function (11) and as an FDA-cleared protocol for depression (12,13). Thus, TBS represents a key intersection of basic neuroplasticity research and translational neuromodulation innovation. Given this importance, it is thus surprising that very little is still known about how TBS modulates single cell activity/excitability when delivered in vivo.

One of the major unexpected and still unexplained findings that emerged from early human TMS research was that the temporal spacing between TBS trains, i.e. the inter-train interval (ITI), is critical in determining the direction of plasticity. In Huang et al.'s original human study (since repeated by others many times), when TBS is repeated with a very short inter-trial interval (2S) there was a net suppression of motor cortex excitability. However, when each 2s TBS was delivered with a longer ITI (10S) there was an enhancement of cortical excitability (2). In other words, short ITIs tend to induce inhibitory effects, while longer ITIs (on the order of 10s) led to facilitation (2,14). This finding has been replicated across human TMS experiments (15) suggesting that the timing structure of TBS trains can modulate direction of excitability (3,5,16–18). Interestingly, this 10s ITI protocol, while generally associated with excitatory outcomes, also exhibits substantial variability across individuals (19), which may reflect a transitional state where excitation and inhibition are closely balanced However, 20 years after the initial report that the ITI drives differences in the direction of TBS induced plasticity (and integration of this finding in both clinical and cognitive neuroscientific workflows), we still do not have a clear mechanistic understanding of why the ITI drives differential plasticity effects.

In this study, using single cell calcium imaging, we probed the effects of electrical stimulation on calcium activity in glutamatergic and GABAergic neurons. We were able to investigate two major hypotheses: 1) cells with elevated levels of calcium influx during TBS are more likely to show long-term plasticity post-stimulation; and 2) increasing the ITI permits the decay of GABAergic activity, resulting in overall net excitation during the TBS protocol and thus overall greater plasticity changes post-stimulation (8). Our findings provide support for these hypotheses. First, we found, across stimulation protocols, that cells with elevated calcium levels are more likely to show a long-term increase in activity post-stimulation, while cells that are suppressed during stimulation are likewise more likely to show a long-term suppression post-stimulation. This effect is weakest at shorter ITIs. Second, we find that shorter ITIs (e.g., 4s and to some extent 10s) led to a greater net increase in calcium levels in GABAergic compared to glutamatergic neurons during stimulation, and were thus associated with weaker and less sustained changes in post-stimulation glutamatergic and GABAergic neurons compared to longer ITIs. By contrast, longer ITIs (especially >20s) produced more balanced neuronal activation dynamics between cell types and resulted in significantly enhanced long-term changes in excitability of both glutamatergic and GABAergic neurons. Histological examination confirmed that shorter ITIs resulted in overall greater relative GABAergic recruitment (particularly in PV cells). Most surprisingly, we found that the "standard" iTBS protocol (the one used across a wealth of human studies, with a 10s ITI) is suboptimal for inducing changes in excitability. Instead, we found that a 20s ITI, henceforth referred to as "extended TBS", produces a maximal increase in

excitability in glutamatergic neurons, while also suppressing activity of GABAergic interneurons. Our results suggest that an adaptation of the classic 10s ITI stimulation protocol to a 20s ITI may improve neuroplastic changes and thus may overall improve the clinical efficacy of TBS.

Results

Divergent Glutamatergic Neuron Responses to Theta Burst Stimulation (TBS). In this study, we investigated two primary questions: (1) How does TBS affect cellular calcium activity both during and after stimulation? (2) How does the inter-train interval (ITI) influence these neuronal responses? To address these questions, we utilized in vivo calcium imaging with a miniaturized microscope to record neuronal activity in the medial prefrontal cortex of rats subjected to TBS stimulation protocols (Fig 1A). Each session consisted of 20 trains of an identical 2S TBS trains with variable ITIs (4 to 60 seconds) (Fig 1B). ITIs was defined from the start of one train to the next, making a 4-second ITI equivalent to a 2-second pause between trains (10S ITI is the standard FDA-cleared clinical protocol). We analyzed the neuronal activity across ~ 1200 cells per ITI condition across 5 rats, which revealed heterogeneous neuronal responses to TBS (Fig 1C). A subset of neurons displayed increased calcium activity relative to baseline, which we classified as 'excited' cells. Conversely, another subset exhibited decreased calcium activity, where were classified as 'inhibited' cells. Some neurons, however, did not show strong modulation following stimulation, which we classified as ‘non-responsive’ cells. We first analyzed whether varying ITIs affected the proportion of glutamatergic cells that were excited vs. inhibited neurons during TBS. We conducted a multi-layer Chi-square test with factors Condition (2 levels: sham, stim), ITI (5 levels), and cell proportion (3 categories: excited, inhibited, non-responsive, Figure 1D). ITI was defined as the covariate, and corrections for multiple comparisons were applied across the five ITIs. For this and other analyses of sham data, only one session of sham was recorded but it was analyzed according to the duration of the comparative ITI window to match the stimulation condition (See method section for more details). Chi-square analysis for overall effect demonstrated significant differences across ITIs in the proportions of both excited ($X^2(1) = 151.15$, $p < 0.0001$) and inhibited cells ($X^2(1) = 11.04$, $p < 0.0001$) between TBS and sham conditions. Post hoc analyses demonstrated significant differences between sham and stimulation conditions exclusively at ITIs 4, 10, and 20, specifically in the proportion of excited cells (ITI 4: $X^2(1) = 103.09$, $p < 0.0001$, ITI 10: $X^2(1) = 42.62$, $p < 0.0001$ ITI 20s: $X^2(1) = 46.89$, $p < 0.0001$, Fig 1E and Table S1). However, we did not see significant differences among inhibited cells (see Table S1 for further stats). Differential plots comparing cell proportions during stimulation versus baseline revealed maximal excitatory shifts at the 4-second ITI (Fig 1F). Thus, TBS at ITIs ≤ 20s significantly increased the proportion of excited glutamatergic cells, but at 40S this effect of stimulation was no longer observed.

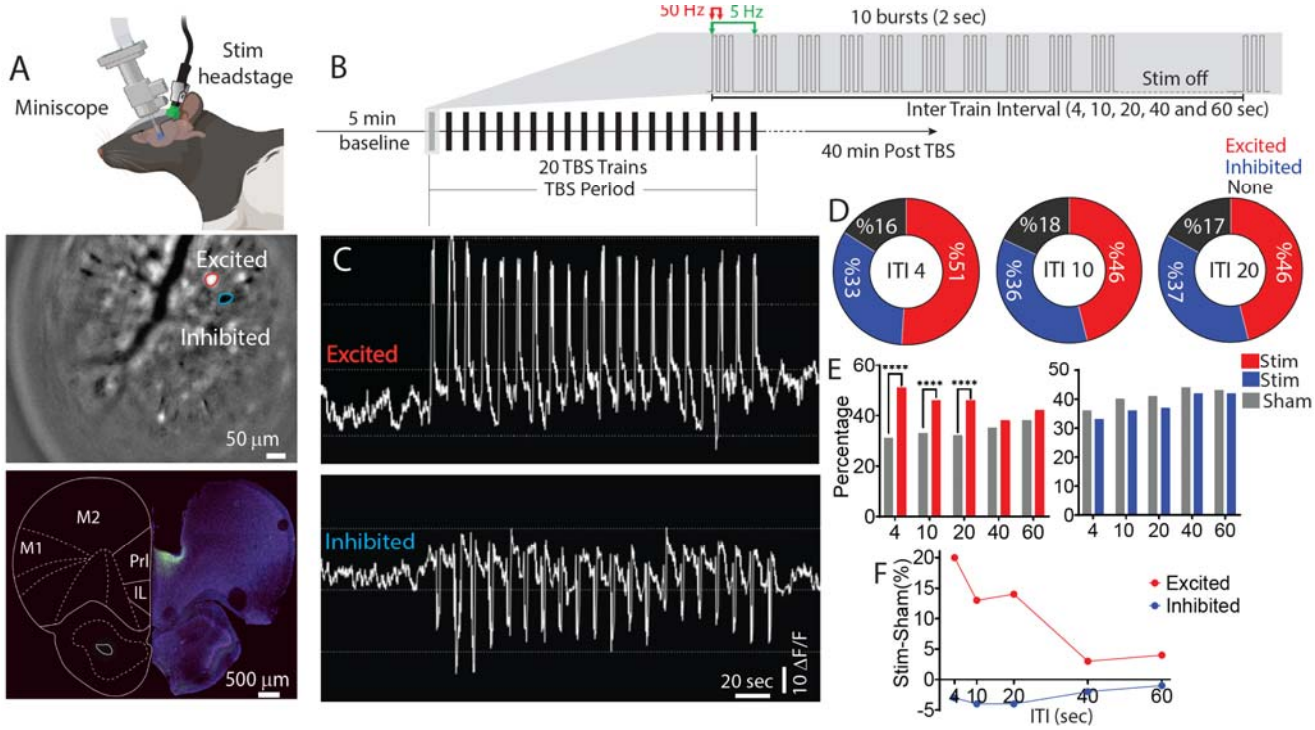

Figure 1. Experimental Design and ITI-Dependent Modulation of Glutamatergic Cortical Cell Responses (A) Schematic of the experimental setup. (Top) Rats were implanted with micro-wires connected to a headstage adapted for electrical stimulation and an Inscopix GRIN lens for single-cell calcium imaging. (Middle) A representative frame from Inscopix data processing showing spatially mapped excited (red) and inhibited (blue) cells within the field of view. (Bottom) Histological verification of CamKII-driven GCaMP expression in the medial prefrontal cortex (green). **(B)** Theta Burst Stimulation (TBS) was delivered as 3 pulses at 50 Hz per burst, with bursts repeating at 5 Hz. Each session included 20 trains, each with 10 bursts. Inter-train intervals (ITIs) were varied (4-60 s) between sessions. Following TBS, calcium imaging continued for 40 minutes. **(C)** Cells were categorized as excited or inhibited and non responsive by comparing their mean activity during 4-second time bins around stimulation trains to baseline levels. **(D)** Short ITIs led to a higher proportion of excited cells and a reduced proportion of inhibited cells during stimulation. **(E)** Chi-square analysis revealed significant differences across ITI in the proportion of excited ($X^2(1) = 151.15$, $p < 0.0001$) and inhibited cells ($X^2(1) = 11.04$, $p < 0.0001$) between TBS and sham conditions. Post hoc analyses indicated that these effects were primarily driven by strong differences between sham and stimulation at ITIs of 4, 10, and 20 seconds (see Table S1 for corrected pairwise comparisons). **(F)** Differential plots of cell proportions (stimulation vs. sham) showed maximal excitatory shifts at ITI 4s, indicating enhanced cell recruitment at shorter intervals. Data is shown as a percentage of the cells. Data were analyzed using Chi-square tests with Sidak's correction for multiple comparisons. Values are reported as mean ± SEM. **$p < 0.0001$; average n ~ 1200 cells per ITI condition across 5 rats.

Extended ITIs Attenuate Excitatory and Inhibitory Calcium Responses in Glutamatergic Neurons During Stimulation. We next examined the effects of TBS on calcium levels directly in the defined populations noted above (excited and inhibited glutamatergic neurons). To quantify this, we examined Z-scored calcium activity across the entire recording session, comparing the responses of excited, inhibited, and all glutamatergic neurons across varying ITIs (Fig 2A-D). We conducted a two-way ANOVA with stimulation condition (sham vs. stim) and ITI as factors. At a population level (i.e. combined across both excited and inhibited neurons) we found a significant main effect of stimulation condition ($F(4, 8998) = 72.65$, $p < 0.0001$), a significant main effect of ITI ($F(4, 8998) = 64.07$, $p < 0.0001$), and a significant interaction between the two factors ($F(1, 8998) = 264.2$, $p < 0.0001$). Post hoc analyses indicated significantly higher population activity during stimulation compared to sham at shorter ITIs ($p < 0.0001$ for

conditions at ITIs 40 and 60. Additionally, there was a significant decline in population-level calcium activity as ITIs were extended from 4 to 60 seconds (Table S2, comparing stimulation conditions directly with each other). No significant differences in calcium activity were found between sham conditions across ITIs. We observed a similar effect when analyzing the sub-population of glutamatergic cells that were excited during stimulation. A two-way ANOVA revealed significant main effects of stimulation ($F(4, 4464) = 86.79$, $p < 0.0001$) and ITI ($F(4, 4464) = 104.8$, $p < 0.0001$), and a significant interaction ($F(1, 4464) = 415.7$, $p < 0.0001$). Post hoc analyses showed elevated calcium responses in the stimulation condition compared to sham across all ITIs ($p < 0.0001$ for ITIs 4, 10, and 20; $p = 0.001$ for ITI 40; $p = 0.008$ for ITI 60), with a progressive decline in activity as ITIs increased. No significant differences were observed between the different sham conditions across ITIs. In the sub-population of glutamatergic cells that were inhibited during stimulation, we found a significant interaction between stimulation and ITI in the opposite direction of what we observed for excited cells. Two-way ANOVA showed a significant main effect of stimulation ($F(4, 4524) = 71.39$, $p < 0.0001$), ITI ($F(4, 4524) = 128.0$, $p < 0.0001$), and a significant interaction effect ($F(1, 4524) = 472.8$, $p < 0.0001$). Post hoc analyses revealed significantly reduced calcium activity in the stimulation condition compared to sham at ITIs 4, 10, 20, and 60 (all $p < 0.0001$), while no significant difference was observed at ITI 40. Sham data for inhibited cells did show significant differences across ITIs, though overall differences were negligible (see Table S2). To visualize the effects of ITI when accounting for sham, we calculated the average stim-sham difference across cell-types and ITIs. The shortest ITI (4 seconds) elicited the largest differences for both glutamatergic cell types (greatest degree of excitation and inhibition) during stimulation, suggesting overall greater neuronal responsiveness to stimulation protocols with a non-linear response that plateaued at 20 seconds (Figure 2F).

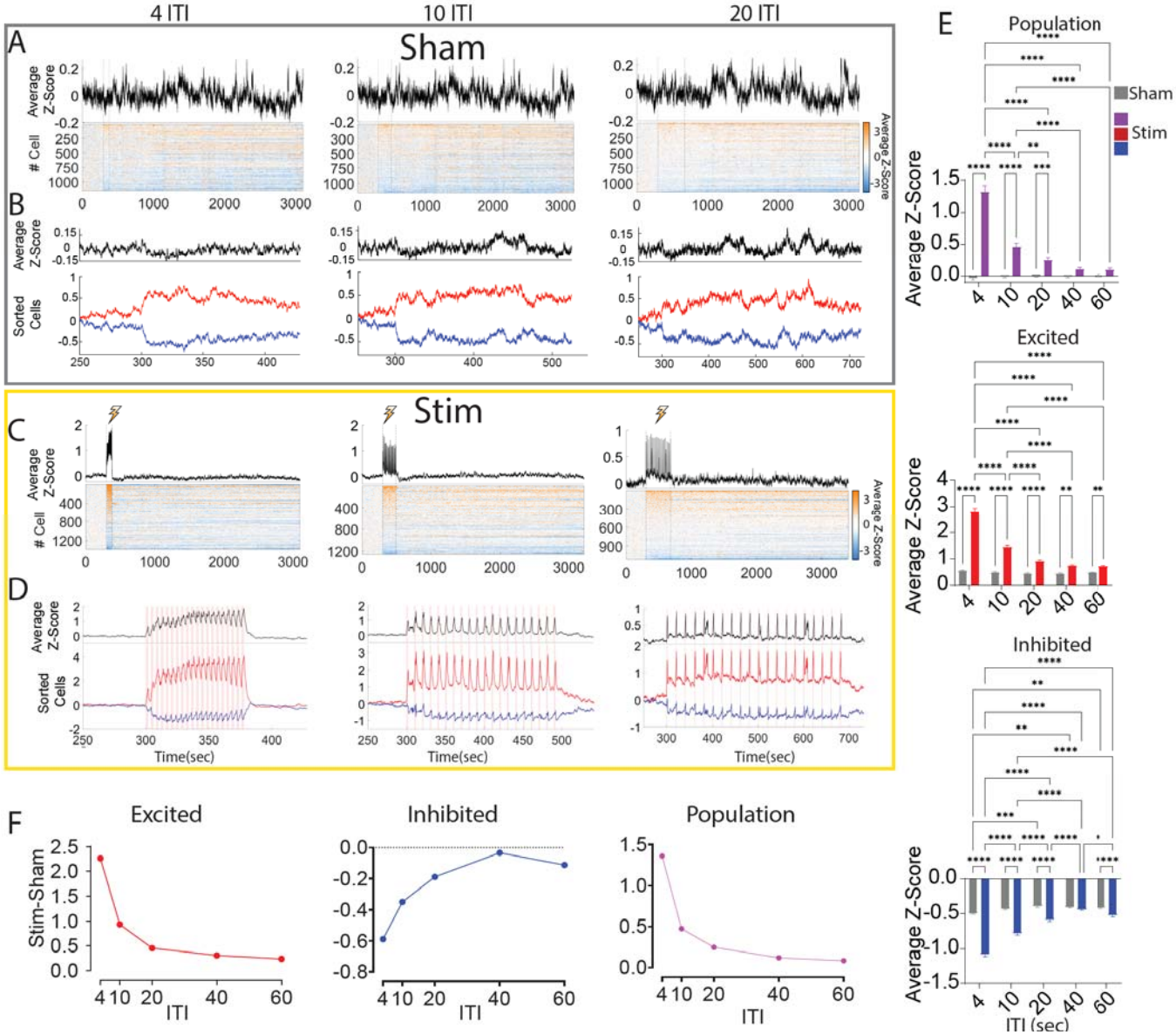
4 ITI
10 ITI
20 ITI
A
Sham
Average Z-Score
Cell
B
Sorted Cells
C
Stim
D
Time(sec)
E
Population
Sham
Stim
Excited
Inhibited
ITI (sec)
F
Stim-Sham
ITI

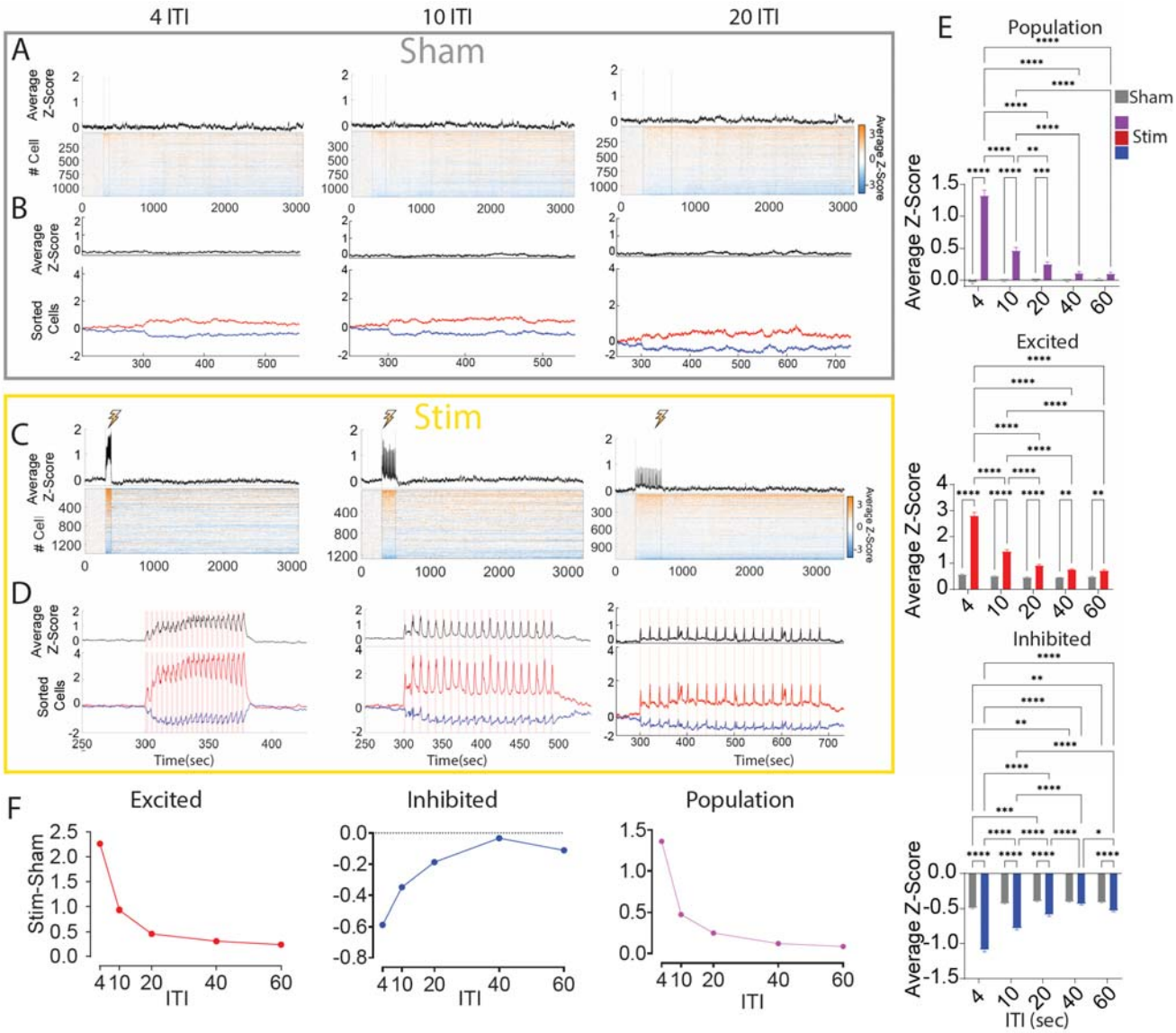

Figure 2. Extended Intervals in Theta Burst Stimulation (eTBS) Reduce Calcium Activity During Stimulation in glutamatergic neurons. (A–D) Z-scored calcium activity across the entire recording session for all recorded cells (top panels, black) and separately for excited (red) and inhibited (blue) subpopulations (bottom panels). Dash vertical lines indicate sham and stimulation periods, respectively. Cells were categorized based on significant changes from baseline activity ($p < 0.01$). Each panel represents a different ITI condition: n = 1384 (ITI 4), n = 1262 (ITI 10), and n = 1119 (ITI 20). **(E)** Average calcium activity during stimulation was compared between sham and stimulation conditions across ITIs, analyzed for excited cells, inhibited cells, and the pooled population. Population-level activity was significantly higher during stimulation than sham at shorter ITIs ($p < 0.0001$ for ITIs 4 and 10; $p = 0.0001$ for ITI 20), but not at ITIs 40 and 60. Across ITIs, population activity declined significantly from ITI 4 to ITI 60 (see Table S2). In excited cells, calcium activity was significantly elevated in stimulation compared to sham at all ITIs ($p < 0.0001$ for ITIs 4, 10, 20; $p = 0.001$ for ITI 40; $p = 0.008$ for ITI 60). However, comparison across ITIs revealed a progressive reduction in activity by extending ITI from 4 to 60. In inhibited cells, stimulation led to significantly reduced activity compared to sham at ITIs 4, 10, 20, and 60 (all $p < 0.0001$), but not at ITI 40. **(F)** Differential plots (stimulus minus sham) for each cell category revealed that ITI 4 produced the strongest increases in excited cell activity, the strongest decreases in inhibited cell activity, and the largest overall population shift. This effect gradually diminished with extending ITI and stabilized into a plateau between ITIs 20 and 60. Data were analyzed using two-way ANOVA followed by Sidak's correction for multiple comparisons. Values are presented as mean ± SEM. *$p < 0.05$, **$p < 0.01$, ***$p < 0.001$, ****$p < 0.0001$.

Extended ITIs Enhance Post-Stimulation Calcium Activity in Glutamatergic Neurons. We next examined how varying inter-train intervals (ITIs) affect post-stimulation effects on glutamatergic excitability. We hypothesized that cells with greater calcium influx during stimulation will show long-term modulation of activity post-stimulation. To explore this, we conducted a two-way ANOVA with stimulation condition (sham vs. stim) and time post-stimulation as factors at each ITI, and separately for cells that were either excited or inhibited during stimulation (as well as at the population level, e.g. both cell types combined). At the full population level, for the short (4S) ITI, we found no main effect of stimulation ($F(1, 15192) = 2.022$, $p = 0.15$), main effect of time ($F(7, 15192) = 0.1878$, $p = 0.98$), or interaction ($F(7, 15192) = 1.427$, $p = 0.189$; Figure 3A). In excited cells (cells excited during stimulation), ITI 4 resulted in a significant decrease in post-stimulation activity ($F(1, 8120) = 57.23$, $p < 0.0001$), with no significant time or interaction effects (Figure 3B). Inhibited cells did not show a significant effect of stimulation. Overall, varying the ITI had a marked impact on the direction of post-stimulation responses, differentially modulating long-term activity in excited versus inhibited cells with shorter ITIs like 4s and 10s showing particularly distinct and informative patterns. By contrast, extended TBS at ITI 20 showed the strongest effects overall. For the full population, there was a main effect of stimulation ($F(1, 13816) = 49.81$, $p < 0.0001$), though no effects of time or interaction (see Table S3 for full statistical details across all ITIs (10S – 40S stimulation protocols all show a significant effect of stimulation). There was also a significant increase in post-TBS calcium activity for excited neurons, ($F(1, 6912) = 53.10$, $p < 0.0001$). Finally, inhibited cells showed both a significant main stimulation effect ($F(1, 6888) = 28.08$, $p<0.0001$) and a main effect of time ($F(7, 6888) = 2.411$, $p=0.01$. Differential plots (stimulus minus sham) revealed a V-shaped profile of post-stimulation effects across ITIs, with a peak and trough at ITI 20 seconds in excited and inhibited populations respectively, as well as a peak for the total population (Figure 3D). This pattern indicates that ITI 20 may represent an optimal interval for maximizing long-term changes in cellular excitability.

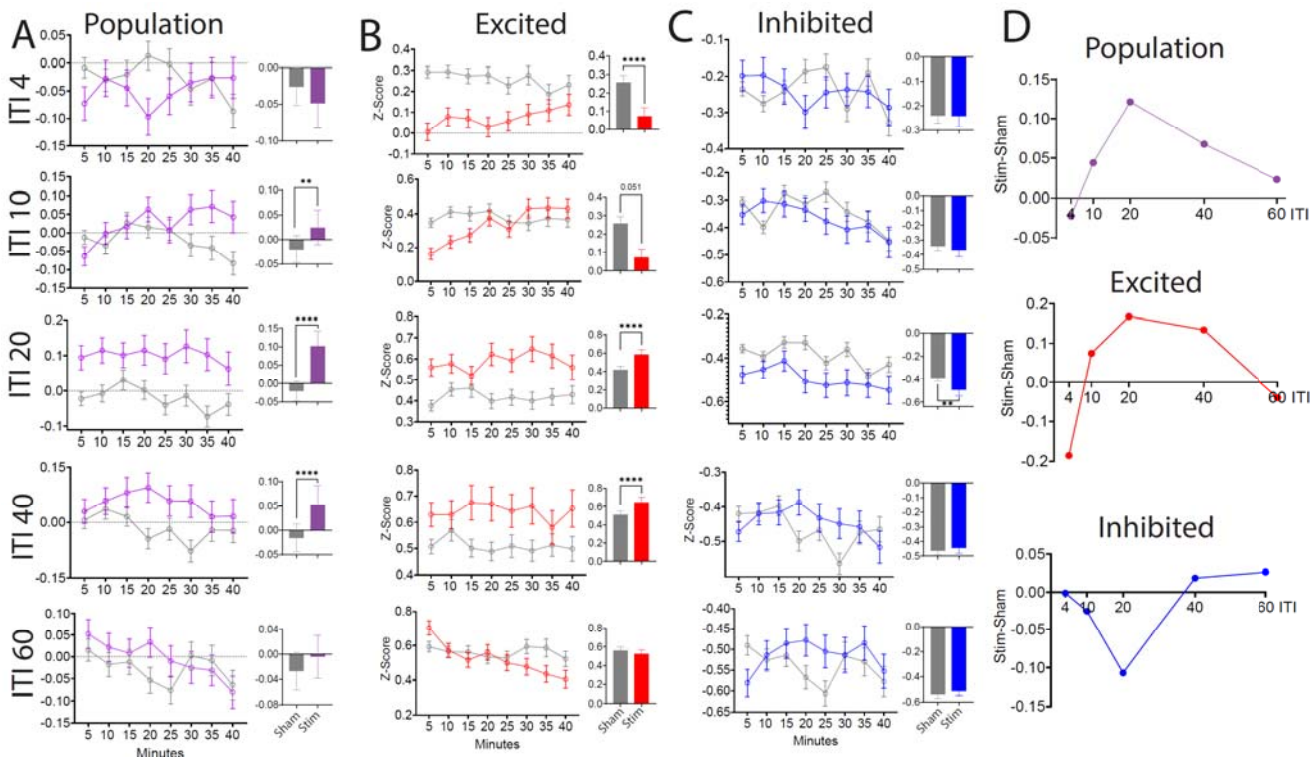

Figure 3. Extended Theta Burst Stimulation (eTBS) Enhances Long-Term Calcium Activity in Glutamatergic Neurons. Cells were classified as excited inhibitedduring TBS by comparing their activity in 4-second bins to baseline activity recorded during the 5 minutes preceding stimulation, using the Wilcoxon rank-sum test ($p < 0.01$). Z-scored calcium activity was calculated by normalizing activity across the session to this baseline. **(A)** Post-TBS Z-scored activity for the pooled population of excited and inhibited cells. A significant long-term increase in calcium activity was observed at ITI 10s ($p = 0.006$), ITI

Bar graphs show the average activity over the full 40-minute post-stimulation period. **(B)** Excited cells showed a significant reduction in post-TBS calcium activity at ITI 4s ($p < 0.0001$). Extending the ITI led to a progressive increase in post-stimulation calcium levels, with a trending effect at ITI 10 ($p = 0.051$) and significant increases at ITIs 20s and 40s (both $p < 0.0001$). **(C)** Other than ITI 20s, inhibited cells did not exhibit significant changes in post-TBS calcium activity compared to sham across any ITI (see Table S3). **(D)** Differential plots (stimulus minus sham) revealed a V-shaped curve in post-stimulation effects across ITIs, with a turning point around ITI 20s seconds, observed in excited, inhibited, and total populations. Data were analyzed using ANOVA followed by Sidak's correction for multiple comparisons. Values are mean ± SEM. *$p < 0.05$, **$p < 0.01$, ***$p < 0.001$, ****$p < 0.0001$. One-sample t-tests against zero: ####$p < 0.0001$.

Extended ITIs Promote Stability of Glutamatergic Neuronal Responses. We next performed several analyses to further clarify the relationships between calcium activity during stimulation and post-stimulation changes in excitability. First, we examined the proportion of excited or inhibited cells that continued to show post-stimulation excitation or inhibition relative to baseline. During sham stimulation, between 57.6% in ITI 4, 66.9% in ITI 10s and 69.1% in ITI 20s of neurons that were excited during the sham stimulation period showed continued elevation of activity post-stimulation (Figure 4A). By contrast, during actual stimulation sessions, we found that shorter ITIs significantly impaired the response consistency. At 4s ITI only 42.9% of neurons excited during stimulation continued to show an increase in activity post-stimulation relative to the baseline. Although cell identity transitions were significantly different across all sham and stimulation conditions ($p < 0.0001$ for all; Figure 4A and B), only the stimulation condition at ITI 4 did not show a significant difference (see Table S4 for details) Thus, at shorter ITIs (4s and 10s), there was active disruption of the process by which cells that were excited during the stimulation period maintained their elevated excitabilities post-stimulation. We next performed a correlation between Z-scored calcium activity during and after TBS (pooling across excited and inhibited cells). Similar to the above analysis, we found that at shorter ITIs (4s and 10s) there was a significantly reduced correlation between activity levels during vs. post TBS relative to the sham group, again suggesting that TBS at shorter ITIs recruits a process that actively prevents plasticity from being sustained beyond the period of stimulation. This process does not occur with ITIs of 20s-60s (Figure 4C-E).

One possible explanation for why shorter ITI impairs plasticity is that too much calcium inside the cell impairs normal processes promoting LTP (20,21). To assess this, within each ITI, we compared calcium activity during the stimulation period from cells that were excited and remain excited vs those that were excited and then become suppressed post-stimulation. We reasoned that if excess calcium impaired plasticity, we would observe more calcium in cells that were suppressed post-stimulation for the shorter ITI paradigms. We did not find this. Instead, we found that across all ITIs (including at the 4S and 10S ITI), cells that remained excited showed higher calcium levels compared to those that become suppressed (Fig 4F-H), and this effect did not differ by ITI (see Table S4 for additional details and statistical analyses). This demonstrates that elevated calcium levels do not impair plasticity, and that other mechanisms are likely responsible for the impaired plasticity with shorter ITI paradigms.

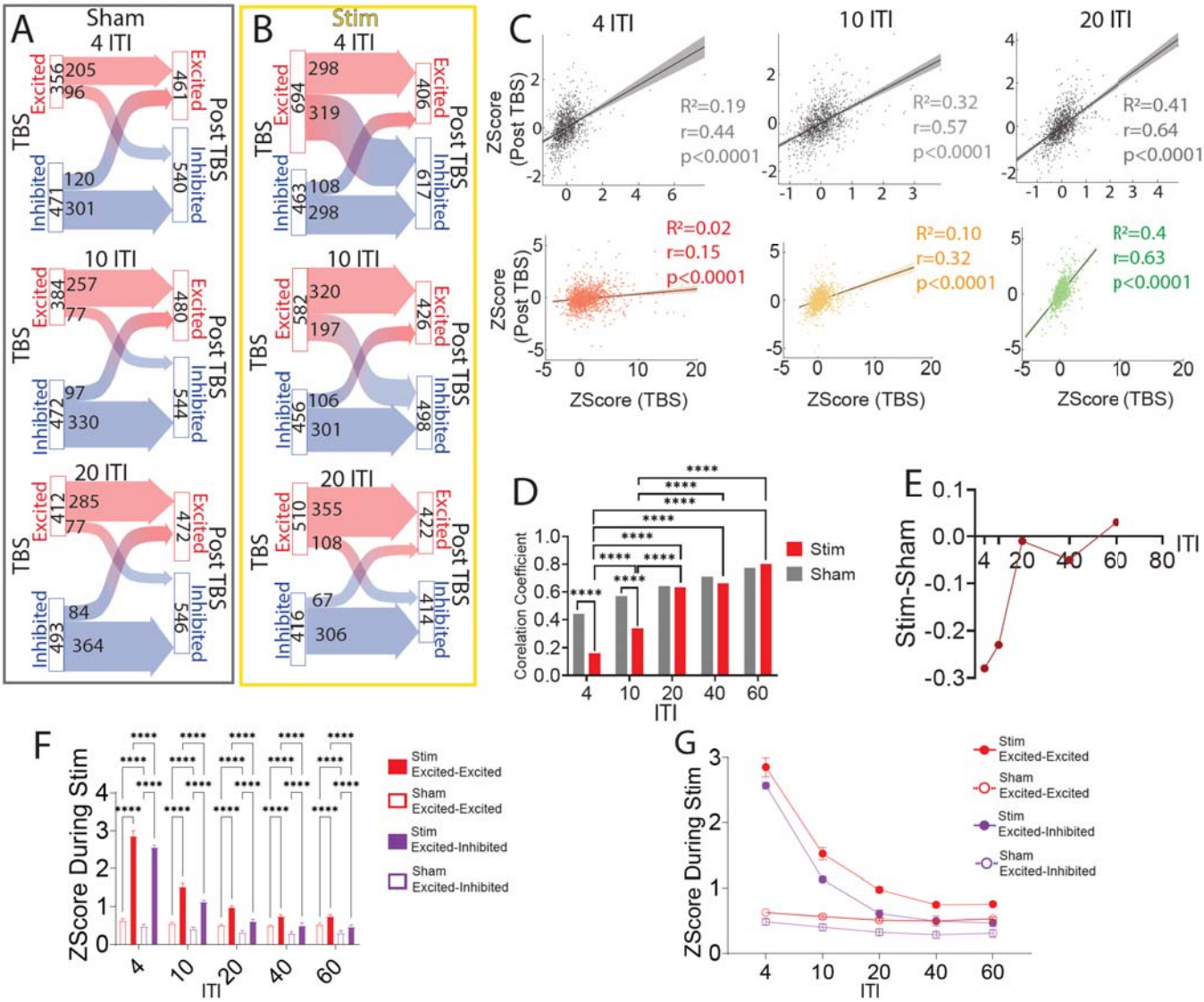

Figure 4. Extended ITIs Promote Stability of Cell Activity and Reduce Activity Transitions Between Stimulation and Post-Stimulation Phases **(A)** Stability of cell activity (excited and inhibited) between TBS and post-TBS periods among sham conditions across ITIs. Cells are color-coded (red: excited, blue: inhibited), and arrow size and shape scale with the number of cells (indicated within shapes). No significant shifts in cell classification were observed across ITIs in sham animals. **(B)** Comparison between stimulation and sham conditions revealed that extended ITIs enhance consistency in excitatory cells. Specifically, fewer cells transitioned from excited during TBS to inhibited post-TBS at longer ITIs. McNemar's test revealed unequal proportions of stable and transitioning cells across all sham and stimulation conditions, except for stimulation at ITI 4 seconds, where the number of stable and transitioning cells was approximately equal. (See Table S4). **(C)** Scatterplots showing the correlation between Z-scored activity during and after TBS for the population (pooled excited and inhibited). **(D)** Extending ITIs significantly increased the correlation between during- and post-TBS activity levels, indicating improved stability of cell responses. **(E)** Comparison of correlation coefficients between stimulation and sham conditions across ITIs showed reduced correlation at short ITIs (ITI 4 and 10, $p < 0.0001$), which recovered to sham levels at extended ITIs (20-60 sec). Differential plots (stim minus sham) indicated equilibrium in during-post correlations emerging at ITI 20. **(F)** Analysis of average calcium activity during stimulation was performed at the level of response-defined subpopulations. These analyses were categorized based on their activity profiles during and after TBS; for example, "excited–excited" cells were excited both during and post-stimulation, whereas "excited–inhibited" cells were excited during but inhibited following stimulation. This analysis revealed that

(G) Consistent with population-level findings, extending ITIs led to a decrease in average calcium levels across all subpopulations during stimulation. Data were analyzed using ANOVA followed by Sidak's correction for multiple comparisons. Linear regression was used for correlation analysis (X = during TBS, Y = post-TBS). Values are mean ± SEM. *$p < 0.05$, **$p < 0.01$, ***$p < 0.001$, ****$p < 0.0001$.

Extended TBS prevents increase of GABAergic activity during stimulation. The above data demonstrated that at shorter ITIs, "inhibited" glutamatergic neurons show greater suppression than at longer ITIs. While there could be several mechanisms underlying this phenomenon, one of them is simply that these neurons are being directly suppressed by GABAergic neurons, which suggests that shorter ITI stimulation recruits greater GABAergic activity. There are several pieces of evidence suggesting that elevated GABAergic activity may affect plasticity. First, many slice studies have shown that GABA receptors (and particularly GABA-B receptors) need to be blocked in order to effectively induce plasticity with TBS protocols (22–24). Similarly, studies in humans have suggested that excess GABAergic agonism can impair plasticity-related clinical effects of stimulation (25). Thus, we hypothesized that shorter ITI TBS paradigms may activate GABAergic neurons, thus limiting plasticity. To directly investigate this, we performed calcium imaging of mDlx-driven GCaMP targeting GABAergic interneurons in a distinct group of animals (Figure 5A). We analyzed data using similar methods as described for glutamatergic cells, in which GABAergic interneurons were categorized as excited or inhibited during stimulation/sham periods (Figure 5B).

We first analyzed whether ITI affected the proportion of GABAergic cells that were activated or inhibited using a multi-layer Chi-square test with factors of stimulation (2 levels: sham, stim), ITI (5 levels), and modulation (3 categories: excited, inhibited, non-responsive, Figure 1C), with multiple comparisons applied across the five ITIs. Chi-square analysis demonstrated significant differences across ITIs in the proportion of excited cells ($\chi^2(1) = 72.24$, $p < 0.0001$), while differences for inhibited cells did not reach significance ($\chi^2(1) = 2.29$, $p = 0.13$) between TBS and sham conditions. Post hoc analyses for excited cells demonstrated the significant effects on excited cells was driven by significant differences between sham and stimulation conditions at shorter ITIs of 4S ($\chi^2(1) = 96.73$, $p < 0.0001$;) and 10S ($\chi^2(1) = 14.06$, $p < 0.0001$) (Figure 5C). No notable differences emerged with extended ITIs (ITI 20–60; see Table S5 for detailed comparisons). To visualize the distribution of effects, we plotted the differences between stim and sham groups in excitation vs. inhibition of GABAergic neurons (Figure 5D). We found that 4s ITI strongly favored activation and 20S ITI produced the most balanced proportion of activation vs. inhibition of GABAergic neurons relative to all other stimulation protocols.

We next examined average calcium activity in GABAergic interneurons during stimulation across ITIs, and compared stimulation and sham conditions within excited, inhibited, and pooled populations. Across all cells, a two-way ANOVA revealed significant main effects of stimulation condition ($F(1, 2512) = 87.39$, $p < 0.0001$), ITI ($F(4, 2512) = 55.25$, $p < 0.0001$), and their interaction ($F(4, 2512) = 52.71$, $p < 0.0001$). Post hoc analyses showed that stimulation produced significantly greater calcium activity compared to sham at shorter ITIs (ITI 4, $p < 0.0001$; ITI 10, $p = 0.006$), with no significant differences at extended ITIs (20–60 sec). Importantly, calcium activity significantly declined from ITI 4 to ITI 20, reaching a plateau thereafter (Figure 5E; Table S6). Within excited GABAergic neurons, two-way ANOVA indicated a significant main effect of stimulation ($F(1, 1250) = 58.25$, $p < 0.0001$), ITI ($F(4, 1250) = 21.20$, $p < 0.0001$), and a significant interaction ($F(4, 1250) = 23.11$, $p < 0.0001$). Post hoc tests revealed significantly elevated calcium levels in stimulation compared to sham at ITIs 4 ($p < 0.0001$) and 10 ($p = 0.002$), alongside progressively declining calcium activity as ITIs increased from 4 to 60 seconds (Table S6). Among inhibited cells, while the main effect of stimulation was significant ($F(1, 1252) = 25.69$, $p < 0.0001$), there were no significant effects for ITI ($F(4, 1252) = 0.79$, $p = 0.53$) or the interaction ($F(4, 1252) = 1.13$, $p = 0.34$). Post hoc analyses revealed significantly reduced calcium activity during stimulation relative to sham at ITIs 4 ($p = 0.003$), 10 ($p = 0.03$), and 40 ($p = 0.033$), with no differences at ITIs 20 or 60. Notably, neither stimulation nor sham conditions showed significant within-group changes across ITIs, emphasizing that observed effects arose specifically from interactions between stimulation condition and ITI duration.

These findings suggest that shorter ITIs (including both 4 and 10S ITI) resulted in significantly greater recruitment of GABAergic cells, both at the level of the proportion of GABAergic cells that get activated

during stimulation and in the mean calcium activity of cells relative to longer ITIs. To better illustrate these effects relative to activation of glutamatergic cells, we plotted the mean difference (stimulation minus sham) in calcium activity across both GABAergic and glutamatergic neurons on the same plot (Fig 5F). We found that at a population level, in TBS up to 20S ITI, there was a net greater activation of GABAergic relative to glutamatergic neurons, which shifted at about 20S ITI. Thus, our results demonstrate that an optimal balance of GABAergic and glutamatergic activation occurs at TBS with 20s ITI. Shorter ITIs resulted in greater GABAergic compared to glutamatergic activation, while longer ITIs minimize GABAergic activation, but also produced lower levels of glutamatergic activation.

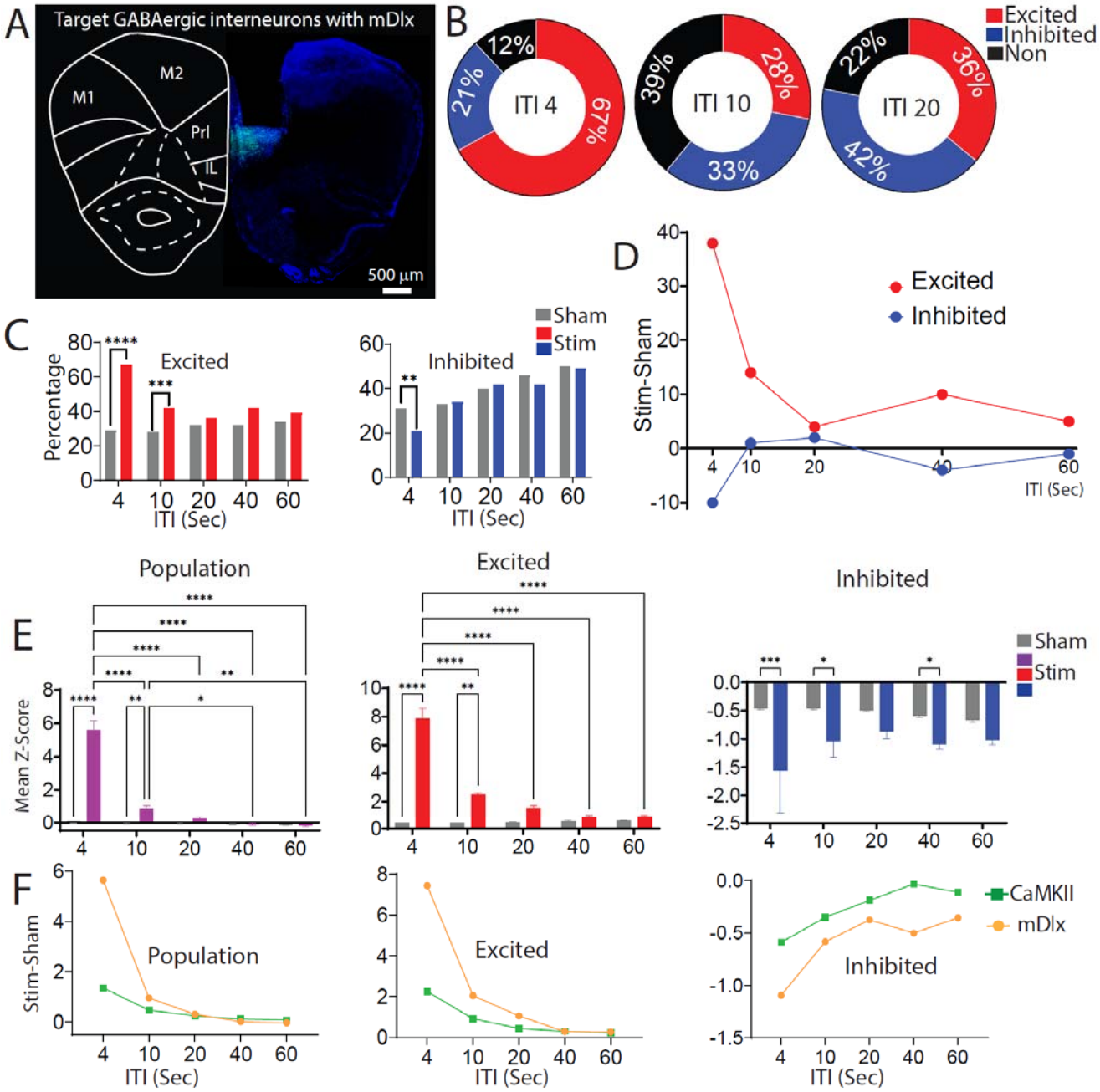

Figure 5. ITI-Dependent Activity of GABAergic Interneurons During Stimulation **(A)** Histological verification of mDlx-driven GCaMP expression in medial prefrontal cortex GABAergic interneurons (green). **(B)** GABAergic interneurons were categorized as excited or inhibited by comparing their mean calcium activity during 4-second time bins around stimulation trains to baseline levels, following

and fewer inhibited cells during stimulation. Chi-square analysis revealed significant differences across ITIs in excited cells ($\chi^2(1) = 72.24$, $p < 0.0001$) but not in inhibited cells. Post hoc analyses showed these differences were driven by significant changes between sham and stimulation conditions at ITIs 4 and 10 (see Table S5 for corrected comparisons). Data presented as cell percentages. **(D)** Differential plots (stimulation minus sham) of cell proportions highlighted maximal excitatory shifts at ITI 4, indicating strong recruitment of GABAergic cells at shorter intervals. Differences gradually diminished with extended ITIs, reaching equilibrium at ITI 20. **(E)** Average calcium activity during stimulation was compared between sham and stimulation conditions across ITIs in excited cells, inhibited cells, and the combined population. Population-level activity was significantly higher during stimulation compared to sham at shorter ITIs (ITI 4: $p < 0.0001$; ITI 10: $p = 0.006$), with no differences at ITIs 20–60. Population activity significantly decreased as ITIs were extended from ITI 4 to ITI 20, thereafter plateauing. In excited cells, calcium activity was significantly higher in stimulation compared to sham at ITIs 4s ($p < 0.0001$) and 10s ($p = 0.002$), with progressively decreasing calcium levels observed as ITIs extended from 4s to 60s (Table S6). In inhibited cells, stimulation significantly reduced activity compared to sham at ITIs 4s ($p = 0.003$), 10s ($p = 0.03$), and 40s ($p = 0.033$), with no significant differences observed at ITIs 20s or 60s. Within-group analyses showed no significant differences across ITIs in either sham or stimulation conditions. **(F)** Differential plots (stim minus sham) comparing glutamatergic (green) and GABAergic (orange) populations. Consistent with glutamatergic neurons, ITI 4 produced robust calcium increases in GABAergic cells, particularly in the excited subgroup. This pronounced effect diminished progressively as ITIs extended, stabilizing between ITIs 20 and 60. Data analyzed by two-way ANOVA followed by Sidak's multiple comparison corrections. Values expressed as mean ± SEM. *$p < 0.05$, **$p < 0.01$, ***$p < 0.001$, ****$p < 0.0001$.

Extended ITIs Induce Sustained Post-Stimulation Suppression of GABAergic Interneurons. We next explored whether TBS ITI affected GABAergic plasticity similarly to what we observed for glutamatergic plasticity. At the population level (pooled across excited and inhibited cells), two-way ANOVA (group × time bin per ITI) did not show significant changes at ITI 4S, but revealed a significant group effect indicating reduced suppression of calcium at ITI > 10s ($p<0.001$ for ITI 10 - 60). At 10s ITI there was an overall reduction in activity of GABAergic neurons post-stimulation compared to sham, but at all other ITIs there was further suppression of calcium in GABAergic neurons compared to sham (Figure 6A; see Table S7 for statistical details). When analyzed separately, excited GABAergic neurons exhibited a significant reduction in calcium activity post-stimulation specifically at the shortest (ITI 4s) and longest (ITI 60) intervals ($p < 0.0001$ for both), with no significant changes at intermediate ITIs (10s, 20s, and 40s; Figure 6B). However, inhibited GABAergic neurons consistently showed highly significant changes compared to sham across all ITIs, displaying a clear ITI-dependent suppression pattern. At short ITIs (4s) GABAergic neurons were significantly less suppressed compared to Sham, however, at all other ITIs they were significantly suppressed compared to sham (Figure 6C). We next plotted differential activity post-stimulation for both GABAergic and glutamatergic neurons (Figure 6D**).** This showed how shorter ITIs (ITI 4s) yielded negligible post-stimulation changes in both glutamatergic and GABAergic subpopulations. Critically, extending ITIs revealed a pronounced divergence at ITI 20s, where maximal post-stimulation enhancement of glutamatergic neurons and maximal suppression of GABAergic interneurons was observed (Figure 6D). This pronounced divergence persisted at longer ITIs albeit with a decay in the glutamatergic population, highlighting ITI 20s as a key interval at which excitatory and inhibitory neuronal activities diverge maximally. Collectively, these results suggest a compelling mechanism to explain the enhanced stability of long-term excitability observed with extended ITIs: less activation of GABAergic neurons during stimulation and pronounced suppression of GABAergic neurons post-stimulation, thus permitting robust and enduring excitatory plasticity within prefrontal cortex.

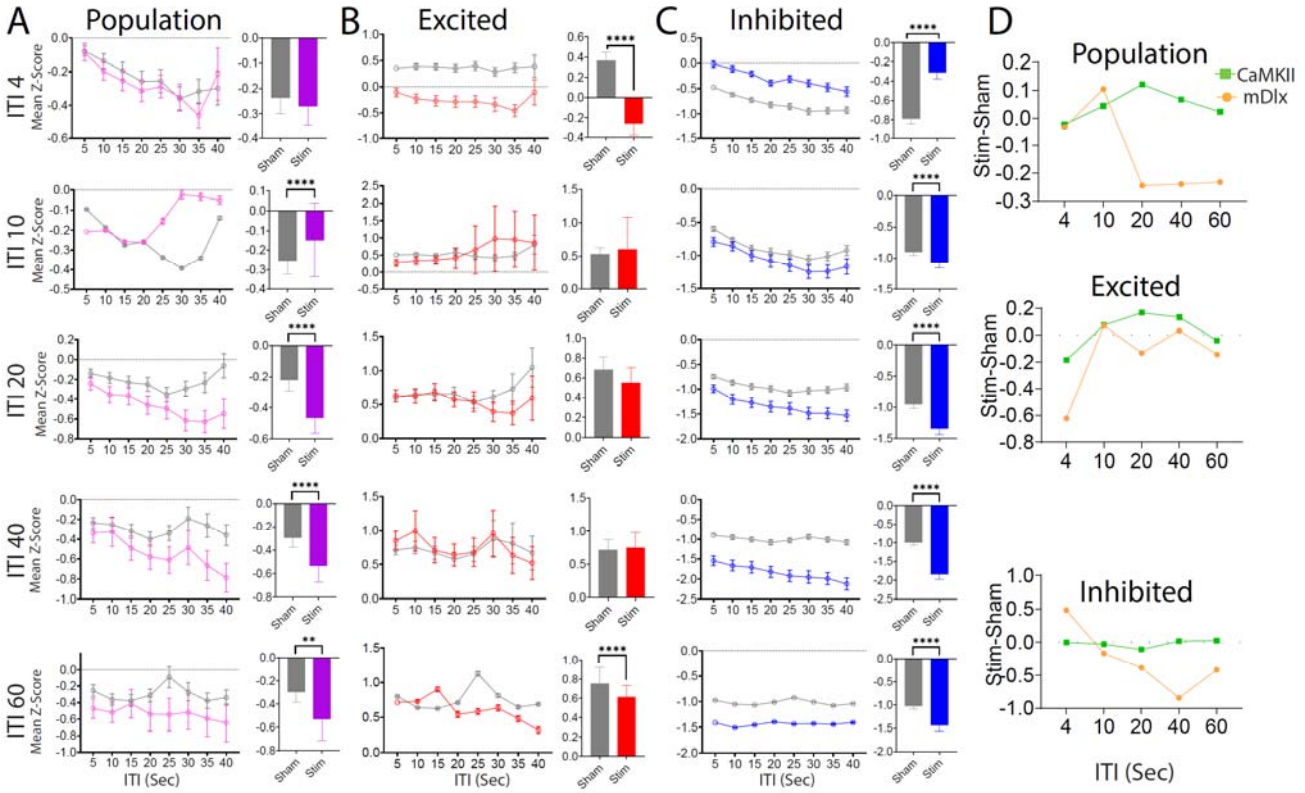

Figure 6. Extended Theta Burst Stimulation (eTBS) Promotes Long-Term Suppression of GABAergic Interneurons. Cells were categorized as excited and inhibited during TBS by comparing their mean calcium activity in 4-second bins around stimulation to baseline levels (5 min preceding TBS), using the Wilcoxon rank-sum test ($p < 0.01$). Z-scored calcium activity was calculated by normalizing cellular activity throughout the session to baseline values. (A) Post-TBS Z-scored calcium activity for pooled populations (combined excited and inhibited cells). Significant long-term increases in calcium activity occurred at ITIs 10 and decrease in 20, and 40 (all $p < 0.0001$), and also significant decrease at ITI 60 compared to sham ($p = 0.0023$). No significant differences were detected at ITI 4. Bar graphs represent mean calcium activity over the entire 40-minute post-stimulation period; significance was assessed via two-way ANOVA (Group × Time bin; see Table S7 and Methods for details). (B) Excited GABAergic neurons exhibited significant reductions in calcium activity post-TBS specifically at ITIs 4 and 60 (both $p < 0.0001$). No significant post-stimulation differences were detected at intermediate ITIs (10, 20, and 40; Table S7). (C) In contrast, inhibited GABAergic neurons showed significant post-TBS activity changes compared to sham across all ITIs, with directionality varying by interval length. Shorter ITIs resulted in reduced suppression, whereas extended ITIs markedly increased suppression ($p < 0.0001$ for all comparisons). (D) Differential plots (stim minus sham) comparing glutamatergic (green) and GABAergic (orange) populations. In line with glutamatergic cells, short ITIs (ITI 4) produced negligible post-stimulation changes in GABAergic subpopulations. However, extending ITIs revealed a pronounced decrease in calcium activity within GABAergic interneurons, notably at ITI 20. This response contrasted sharply with glutamatergic neurons, which reached peak enhancement at the same interval. Thus, ITI 20 represents a critical point at which glutamatergic and GABAergic post-stimulation calcium responses diverge most substantially. Data were analyzed using ANOVA followed by Sidak's correction for multiple comparisons. Values are mean ± SEM. *$p < 0.05$, **$p < 0.01$, ***$p < 0.001$, ****$p < 0.0001$.

Extending ITI Increases c-Fos Expression but Does Not Sustain Increased GAD-65 Levels in GABAergic Interneurons. To further clarify the cellular mechanisms underlying the differential excitatory and inhibitory dynamics induced by varying ITIs during TBS, we examined molecular indicators of neuronal activation and inhibitory neurotransmission. In a separate cohort of rats, we stimulated the medial prefrontal cortex (mPFC) at short (4S), standard (10S), and extended (20S) ITIs, and evaluated subsequent neuronal excitability by quantifying c-Fos, an immediate-early gene marker widely recognized to reflect neuronal

stimulation condition ($F(3, 36) = 8.342$, $p = 0.0002$), region of interest: ROI ($F(2, 36) = 28.22$, $p < 0.0001$), and a significant interaction between these two factors ($F(6, 36) = 3.381$, $p = 0.0095$; Figure 7A–B). Post-hoc analysis indicated that the short ITI (4S) induced the highest c-Fos expression, particularly within the region closest to the stimulation electrode (ROI 1), compared to the extended ITI (20 s; $p = 0.02$) and sham conditions ($p < 0.0001$). To examine within-group ROI differences, we conducted a one-way ANOVA across the three ROIs. Results confirmed significant ROI-dependent differences in stimulated conditions for ITI 4 ($F(2, 9) = 13.45$, $p = 0.002$), ITI 10 ($F(2, 9) = 9.424$, $p = 0.006$), and ITI 20 ($F(2, 9) = 7.017$, $p = 0.01$), but not in sham animals ($F(2, 9) = 0.3499$, $p = 0.71$). Thus, consistent with physiology results, we find that TBS at all ITI intervals results in focal changes in neuronal activation (ROI effect), with 4S ITI also showing greater overall activation relative to the 20S ITI.

Next we assessed the expression of glutamic acid decarboxylase-65 (GAD-65), an enzyme critical for synthesizing GABA and that is linked to both inhibitory neurotransmission strength and GABAergic neuronal activity (27). Immunofluorescence analysis revealed significant ITI-dependent changes in GAD-65 expression. Our analyses indicated robust main effects of stimulation condition ($F(3, 36) = 78.19$, $p < 0.0001$), ROI ($F(2, 36) = 18.33$, $p < 0.0001$), and their interaction ($F(6, 36) = 7.231$, $p < 0.0001$). The short ITI (4 s) evoked significantly higher GAD-65 expression compared to the extended ITIs (ITI 10 and 20, both $p < 0.0001$) and sham conditions ($p < 0.0001$). Moreover, a one-way ANOVA comparing ROIs (Fig 7C) revealed significant ROI differences within ITI 4 ($F(2, 9) = 11.84$, $p = 0.003$) and ITI 10 ($F(2, 9) = 7.436$, $p = 0.012$), whereas no significant ROI differences were detected at ITI 20 ($F(2, 9) = 2.042$, $p = 0.185$) or sham ($F(2, 9) = 0.0088$, $p = 0.99$). Additionally, extending the ITI to 20S produced no significant differences in GAD-65 levels compared to sham conditions, suggesting a return toward baseline inhibitory enzyme expression with prolonged intertrain intervals.

Given the complexity and functional heterogeneity of cortical GABAergic interneurons, we next attempted to determine whether specific interneuron subpopulations differentially contribute to the observed variations in inhibitory signaling. Previous studies have identified multiple interneuron subtypes with distinct physiological profiles and circuit functions, including parvalbumin (PV)-expressing interneurons (fast-spiking) and somatostatin (SST)-expressing interneurons (slow-spiking) as major modulators of cortical excitability and plasticity (28,29). We therefore quantified colocalization of GAD-65 specifically within these two interneuron subtypes using triple immunofluorescence staining and confocal microscopy (Figure 7D–E). Colocalization analysis was conducted using Mander's coefficients. Two-way ANOVA (stimulation condition × cell type) revealed significant main effects of stimulation condition ($F(3, 24) = 29.10$, $p < 0.0001$), cell type ($F(1, 24) = 76.95$, $p < 0.0001$), and a trending interaction effect ($F(3, 24) = 2.834$, $p = 0.059$). Post hoc analyses indicated that across all stimulation and sham conditions, GAD-65 was consistently more prevalent in PV compared to SST interneurons (ITI 4: $p < 0.0001$, ITI 10: $p = 0.0001$, ITI 20: $p = 0.004$, Sham: $p = 0.004$). Between stimulation conditions, this difference was significantly amplified at ITI 4, indicating stronger responsiveness of PV interneurons to brief stimulation intervals (ITI 4 vs. sham: $p < 0.0001$; ITI 4 vs. ITI 10: $p = 0.0002$; ITI 4 vs. ITI 20: $p < 0.0001$; ITI 10 vs. sham: $p = 0.029$). Similarly, SST interneurons also showed amplified GAD-65 colocalization at ITI 4 compared to sham ($p = 0.0008$), ITI 10 ($p = 0.035$), and ITI 20 ($p = 0.022$). However, no significant differences between ITI 10, ITI 20, and sham were detected in SST cells. Thus, longer ITIs progressively reduced these colocalization differences, with ITI 20 patterns resembling Sham.

We finally questioned whether the enhanced GAD-65 colocalization observed in PV interneurons necessarily reflects greater GABA production or release compared to SST interneurons. To directly address this, we analyzed intracellular intensity of GAD-65 within individually reconstructed PV and SST cells (Figure 7F–G). Two-way ANOVA (stimulation condition × cell type) indicated significant main effects of stimulation condition ($F(3, 24) = 25.71$, $p < 0.0001$) and cell type ($F(1, 24) = 12.13$, $p = 0.0019$), but no significant interaction ($F(3, 24) = 0.686$, $p = 0.56$). Post hoc analysis showed significantly higher GAD-65 intensity within PV interneurons compared to SST at short ITIs (ITI 4 and ITI 10, both $p = 0.02$), with no significant differences at extended ITI (20 s; $p = 0.4$) or sham ($p = 0.23$). Intracellular GAD-65 intensity in PV neurons peaked at ITI 4 compared to all other conditions (ITI 4 vs. ITI 10: $p = 0.013$; ITI 4 vs. ITI 20 and sham: $p < 0.0001$; ITI 10 vs. sham: $p = 0.03$). Similarly, SST neurons also displayed increased GAD-65 intensity at ITI 4 relative to ITI 10 ($p = 0.016$), ITI 20 ($p = 0.0014$), and sham ($p = 0.0002$), though these

changes were less pronounced than in PV cells. No significant differences were detected among ITI 10, ITI 20, and sham for either cell type. Thus, shorter intervals drive stronger activation of GABAergic interneurons, particularly PV cells, while extended ITIs are indistinguishable from sham stimulation protocols.

Taken together, our findings provide critical cellular insight into ITI-dependent modulation of cortical excitability and inhibition. Short ITIs increased overall neuronal excitability (indicated by elevated c-Fos) with pronounced activation of GABAergic interneurons, especially PV interneurons. Conversely, extended ITIs balanced neuronal activity by restoring inhibitory signaling to baseline, offering a plausible cellular mechanism underlying enhanced stability of cortical plasticity at longer intervals.

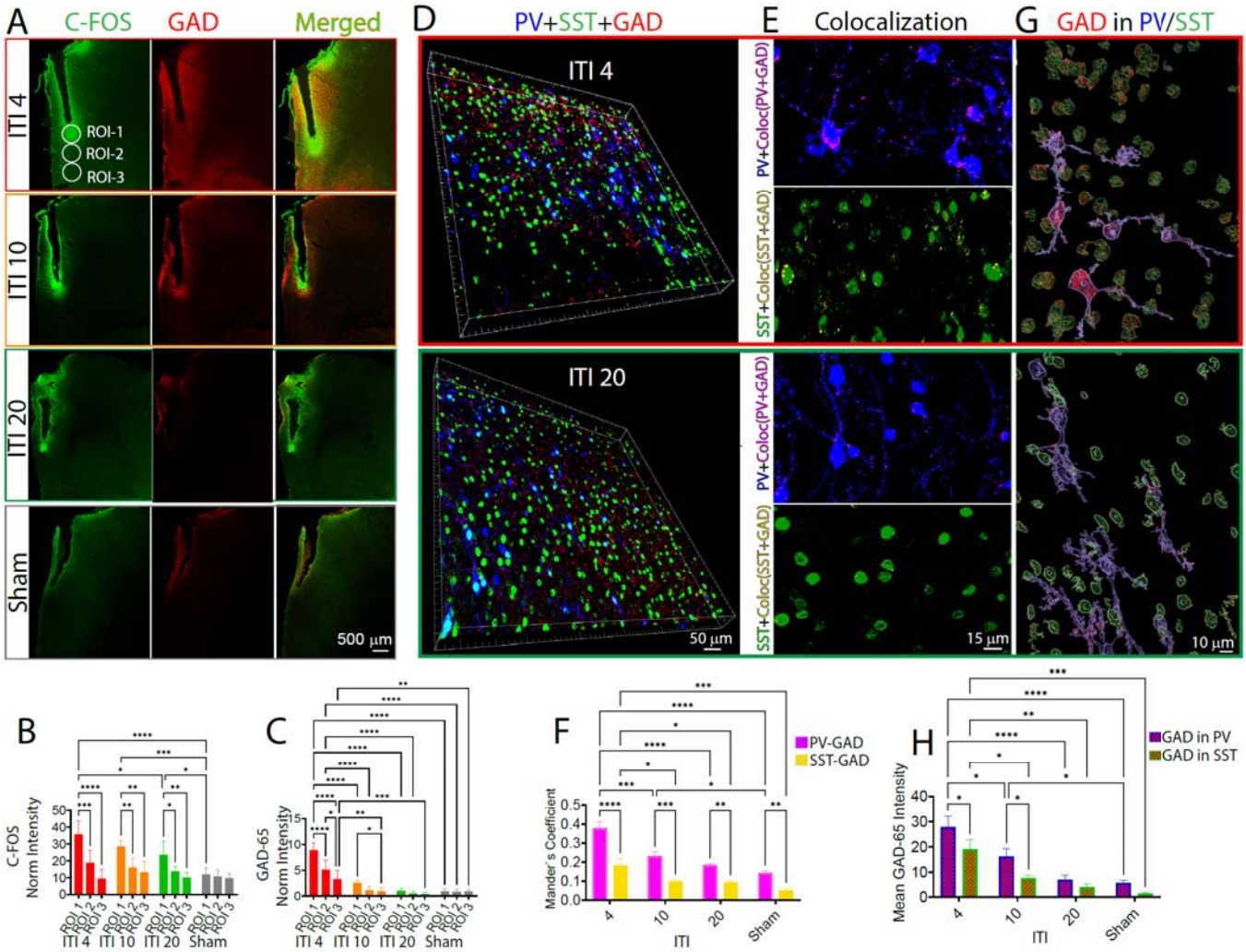

Figure 7. Immunohistochemical Analysis of c-Fos and GAD-65 Expression in Response to Different ITIs of Theta Burst Stimulation. (A) Representative example of double staining for c-Fos (green) and GAD-65 (red). Sham animals underwent electrode implantation and were connected to the stimulator but received no stimulation. euthanized and data were collected 60 minutes post-stimulation. White circles denote regions of interest (ROIs), spanning 500 µm ventral the stimulation electrode. **(B)** Quantification of c-Fos expression across ITIs and sham revealed significant effects for group ($p = 0.0002$), ITI ($p < 0.0001$), and their interaction ($p = 0.0095$). ITI 4 produced the highest c-Fos expression in ROI 1 compared to the extended ITI at 20 s and sham. Statistical comparisons across ROIs within the stimulation groups revealed significant ROI differences for stimulated animals but not sham. Asterisks for between-group differences across ITIs/sham are not shown for clarity. **(C)** Quantification of GAD-65 expression showed significant main effects for group, ITI, and their interaction (all $p < 0.0001$). Similar to c-Fos, GAD-65 expression was highest at short ITI (ITI 4), significantly greater compared to extended ITIs and sham. However, unlike c-Fos, significant differences in GAD-65 levels were observed across multiple ROIs at shorter ITIs, rather

Magnified representative 3D reconstruction from ROI 1 using Imaris software, demonstrating triple immunostaining: SST (green), PV (blue), and GAD-65 (red). **(E)** Representative example of colocalization analysis using Mander's coefficients quantified the overlap of GAD-65 with PV and SST interneurons. **(F)** Generally, GAD-65 colocalization was greater with PV than SST neurons, even in sham animals. This uneven distribution increased further at short ITIs (ITI 4) but decreased progressively with extended ITIs. ITI 20 closely matched sham in colocalization levels. Significant differences in GAD-65-PV colocalization were observed between ITI 4 and all extended ITIs and sham. ITI 10 showed significantly greater GAD-65 colocalization in PV neurons compared to sham ($p = 0.02$), with no significant differences in SST neurons. ITI 20 did not differ significantly from sham in colocalization levels for either SST or PV neurons. **(G)** Zoomed-in representative example of 3D cellular reconstruction generated with Imaris (surface module), showing SST (green) and PV (blue) neurons. GAD-65 intensity within cells is depicted in red. **(H)** Quantification of GAD-65 intensity inside individual SST and PV cells (averaged per animal). At short ITIs (ITI 4 and ITI 10), GAD-65 intensity was significantly greater within PV compared to SST neurons ($p = 0.02$ for both ITIs), while no significant cell-type differences were detected for ITI 20 or sham. Furthermore, GAD-65 intensity inside both SST and PV neurons at ITI 4 was significantly higher compared to ITI 10, ITI 20, and sham. No significant differences were found between ITI 20 and sham, indicating a return to baseline levels at extended intervals. Data were analyzed using ANOVA followed by Sidak's correction for multiple comparisons. Values represent mean ± SEM, n = 4 rats per group. *$p < 0.05$, **$p < 0.01$, ***$p < 0.001$, ****$p < 0.0001$.

Discussion

This study provides single-cell evidence that the timing of theta burst stimulation (TBS) trains critically governs excitatory (glutamatergic) and inhibitory (GABAergic) neuron dynamics in rat prefrontal cortex. Short inter-train intervals (e.g. 4s) induced an immediate surge of calcium activity in both glutamatergic and PV-GABAergic neurons during stimulation, whereas extended ITIs (20s) yielded modest but significant activation of glutamatergic cells and, importantly, minimal activation of GABAergic cells. We found that TBS with an ITI of 20s emerged as a "sweet spot" that maximized long-term activation of glutamatergic neurons, potentially through suppression of GABAergic neurons, maximizing plasticity overall (1–3). This represents the first systematic, single-cell analysis across a range of ITIs in both excitatory and inhibitory cortical neurons, shedding light on how patterned stimulation timing can toggle neural circuits between potentiated and depressed states.

Different ITIs change Excitation/Inhibition balance and may have long term effects on plasticity

It is well established that the pattern of stimulation, including pulse frequency, duration and ITI, critically modulates calcium dynamics and determines plasticity outcomes in cortical circuits (11, 7, 8). For example, Huang et al. (2005) first demonstrated in humans that a continuous 40 s TBS (cTBS with no ITI; 600 pulses) suppressed cortical excitability, whereas the same number of pulses in the same burst pattern, when delivered in trains of 2s spaced by 10s intervals (identical to our ITI 10s protocol), enhanced excitability (7). Our results with electrical stimulation in rodents align with these findings and provide novel insight into the mechanisms whereby ITI determines the direction and stability of plasticity following TBS (7).

We observed that short ITIs strongly increased calcium activity in both glutamatergic and GABAergic neurons during stimulation. The rapid recruitment of interneurons at ITI 4s enhances inhibitory tone, contributing to rapid attenuation of glutamatergic neuron activity post-stimulation (9,30). Fast-spiking interneurons are known to fire at high rates in response to synchronous excitatory input, thereby constraining excitatory outputs (28,31,32). This implies that dense stimulation bursts with minimal time between trains powerfully drives feedback and inhibition in cortex. Indeed, in both human and animal cortex, continuous TBS has been shown to engage inhibitory circuits so strongly that it produces net suppression of excitability (7,8,38), likely via intense interneuron activation. Another possible contributor to reduced glutamatergic excitation is that near-continuous pulses at short ITIs trigger high levels of calcium in excitatory neurons, resulting in synaptic fatigue, impairing normal synaptic function and limiting further neurotransmission (33,34). However, our results suggest that high levels of intracellular calcium are associated with sustained neuronal activation, independent of ITI, and that altered activity following TBS is primarily due to changes in the E/I balance (35,36).

In contrast, extended ITIs (particularly between 20-40s) resulted in sustained activation of glutamatergic neurons and a pronounced suppression of GABAergic interneuron activity in the long term. Therefore, it appears that spaced TBS not only avoids over-driving interneurons during stimulation but also induces a lasting reduction in their post-stimulation activity. Functionally, this can be viewed as long-term disinhibition, a weakening of inhibitory tone that would favor increased network excitability. There is precedent for such inhibitory plasticity: repetitive theta-bursts can trigger lasting decreases in GABA release or interneuron firing, mediated by mechanisms such as GABA-B auto receptor activation or long-term depression at interneuron synapses (9,22,30). This phenomenon provides a compelling explanation for the stable LTP-like excitatory potentiation we observed at ITI 20. If interneurons are persistently less active, pyramidal cells can fire more freely and maintain elevated activity (37,38). In essence, extended ITIs may embed a form of long-term depression (LTD) in inhibitory cortical circuits. This mechanistic interpretation is supported by prior in vivo studies: Benali et al. (2011) found that intermittent TBS (with 10 s pauses) increased markers of excitatory plasticity and cortical output, whereas continuous TBS induced more inhibitory effects (9). Interestingly, iTBS is not unique in modulating both inhibitory and excitatory synapses: in rat brain slices, 10 Hz rMS (no cranium) induces LTP at excitatory synapses and LTD in inhibitory synapses on pyramidal neurons (39, 40). These results align with literature showing that disinhibition is a key requirement for consolidating LTP more generally (9,41). Pharmacological studies have long shown that blocking GABA receptors permits or amplifies LTP induction (30,42). Conversely, if inhibition is triggered during high-frequency or continuous stimulation, it can lead to LTD or no potentiation (22,43).

Although not directly examined in the present experiments, TBS protocols have also been shown to elicit metaplasticity, which adjusts the threshold for inducing plasticity in a direction that stabilizes overall network function (44). Evidence for TBS-induced metaplasticity comes from studies that "prime" the brain using TBS to influence the subsequent response to rTMS. For instance, administering subthreshold rTMS prior to TBS can alter the direction and magnitude of TBS effects (45). Priming effects have also been reported within a single session of TBS, with each train influencing the outcome of subsequent ones (46–49). Overall, the length of the ITI in TBS paradigms (including continuous TBS) may trigger conflicting changes in the E/I balance, potentially in combination with mechanisms such as metaplasticity to impair long lasting plasticity (35,36).

Key role of interneurons in TBS

To further dissect interneuron contributions, we examined two major subtypes: parvalbumin-expressing (PV) and somatostatin-expressing (SST) interneurons. Our immunohistochemical data revealed differential responses of PV and SST cells to TBS timing. At short ITI (4 s), PV interneurons showed significantly greater activation and GABA synthesis engagement than SST interneurons, as evidenced by higher elevated GAD-65 (glutamate decarboxylase) intensity in PV cells, whereas no differences were observed in the 20s ITI eTBS. In other words, fast-spiking PV interneurons appeared to be the primary drivers of the intense inhibitory response under short ITI TBS protocols (28,50). PV interneurons are well-known for their ability to fire at high frequencies with precise timing and minimal adaptation and target the perisomatic region of pyramidal cells to provide powerful inhibition (9,28). Their intrinsic properties (low input resistance, fast membrane kinetics) essentially make them “synchrony detectors” that preferentially respond to the kind of tightly clustered input that short-interval TBS provides (51). Once recruited, PV neurons can rapidly release GABA and strongly curtail pyramidal cell spiking. Our finding that PV neurons had increased GAD-65 levels at ITI 4 indicates they were actively producing/releasing GABA at high levels during and immediately after stimulation. Importantly, as the ITI was extended, the PV interneuron engagement diminished by ITI 20 s, showing GAD-65 levels comparable to sham. This indicates that spaced bursts no longer preferentially hyperactivate PV cells (9). Consequently, the strong inhibitory influence seen with short ITIs (of <20 s) is alleviated at extended ITI (20 s). We propose that PV interneurons are the key mediators of ITI-dependent inhibition: when bursts are too close together, PV cells fire persistently and enforce a high inhibitory tone (thereby limiting net excitation), but when bursts are spaced, PV cells do not reach the same level of sustained firing, allowing excitatory neurons to escape their grip. Prior literature supports this view; PV

interneurons have been implicated in controlling the gain and timing of network excitation, effectively creating a “ceiling” on pyramidal cell activity during intense stimulation (9,28).

Our data further suggest that SST interneurons might contribute to longer-term effects: for instance, SST cells often inhibit other interneurons (including PV cells) and can thus provide disinhibition in a delayed fashion (28,29). It is conceivable that with extended ITIs, SST interneurons (or other non-PV subtypes) gradually modulate the circuit to keep PV activity in check, promoting the prolonged disinhibition we observed post-TBS. The exact interplay between PV and SST populations in our paradigm will require further investigation, but our findings clearly indicate that PV interneurons are more responsive to brief ITIs and likely drive the acute inhibitory feedback that distinguishes short vs. spaced TBS. The preferential activation of PV cells at short ITI is congruent with observations by Benali et al. (2011) that iTBS paradigms reduce PV expression presumably because PV cells were highly active and then subsequently downregulated (9). PV neurons have been implicated in the response to rTMS in a wide range of animal models, with evidence for local and network wide effects (52,53). Future studies using targeted in vivo patch-clamp recordings or optogenetic tagging of PV and SST interneurons during varying TBS protocols could directly test the dynamic firing properties and synaptic responses of these subtypes. This would clarify the circuit-level causal relationships between interneuron recruitment, GABA release, and pyramidal neuron plasticity. Additionally, calcium imaging with genetically encoded neurotransmitter sensors or photometry combined with pharmacological blockade of GABA-A or GABA-B receptors could help parse the contribution of distinct inhibitory mechanisms to ITI-dependent effects. Finally, expanding this framework to other cortical regions or behavioral tasks would determine whether extended ITI stimulation can enhance learning or therapeutic outcomes, offering translational relevance for refining clinical TBS applications.

Is there an optimal ITI for iTBS?

The U-shaped relationship we observed with little long-term change at the extremes (4 s or 60 s) but maximal potentiation at 20-40s implies that two competing processes are at play. At very short ITIs, inhibitory and metaplastic processes likely accumulate and restrict plasticity. Our results show that extending the ITI progressively reduced the peak calcium response during TBS, which is in line with the idea that longer pauses between bursts allow partial dissipation of excitatory build-up and prevent full summation, minimizing metaplastic mechanisms and allowing for sustained plasticity changes. However, at extremely long ITIs (60 s), each burst train may act in isolation, failing to build up the postsynaptic calcium or kinase signaling cascades needed for sustained LTP (3,54,55).

Our differential analysis suggests a “sweet spot” at ITI 20s: excitatory neurons showed peak enhancement while inhibitory neurons showed peak suppression (Figure 6D). The sustained glutamatergic activation we observed with ITI 20s likely reflects this optimal excitatory/inhibitory interplay, where excitatory neurons receive repetitive depolarizing bursts that are not prematurely quenched by inhibition, enabling synaptic strengthening processes. In contrast, at ITI 10s, the inhibitory and excitatory changes seem to cancel each other out and this may contribute to the variability seen in human experiments. In a situation where ITI 10s has similar effects on excitatory and inhibitory neuronal activity, individual baseline E/I balance may have a deciding influence on the outcomes of stimulation. In support of the possibility, baseline cortical excitability has been identified as a predictor of response to iTBS (ITI 10s) not only in healthy participants, but also in people with depression receiving treatment with iTBS (56–58)(refs).

Conclusion

In conclusion, our results collectively suggest that the stability of neuronal responses following extended ITIs arises from a balanced convergence of glutamatergic and GABAergic activity. Short ITIs, despite inducing robust immediate responses, disrupt long-term equilibrium, possibly due to an imbalance in E/I dynamics. Conversely, moderate ITIs, particularly around 20 seconds, promote an optimal interaction between excitatory and inhibitory neuronal populations, fostering sustained post-stimulation stability. This mechanistic insight significantly clarifies how extended intervals between theta bursts modulate enduring cortical plasticity and stability. Our findings suggest ways to reduce variability with current iTBS protocols, and potentially improve therapeutic efficacy/reliability of iTBS by extending the ITI in order to maximise the excitation response.

Stars Methods

Resource Availability

Further information and requests for resources should be directed to and will be fulfilled by the Lead Contact, Dhakshin Ramanathan (email: dramanathan@health.ucsd.edu) and Morteza Salimi (email: msalimi@health.ucsd.edu)

Materials Availability

This study did not generate new unique reagents.

Data and Code Availability

Data and code used in this study are available upon reasonable request from the Lead Contact.

Experimental Model and Subject Details

Animals

Adult male Long-Evans rats (250–300g) were used in all experiments. Animals were housed under a 12:12 light/dark cycle with ad libitum access to food and water. All procedures were approved by the Institutional Animal Care and Use Committee (IACUC) at San Diego VA Medical Center IACUC (Protocol Number A12-021).

Method Details

Virus Injection and Miniscope Implantation

To label excitatory or inhibitory neurons, rats were injected with AAV-Syn-GCaMP for glutamatergic neuron imaging or AAV-Dlx-GCaMP for GABAergic imaging. A GRIN lens was implanted above the medial prefrontal cortex for calcium imaging using a Inscopix miniaturized one-photon microscope.

Theta Burst Stimulation Protocols

TBS consisted of 20 trains of 2-second bursts (3 pulses at 50Hz repeated at 5Hz) delivered via implanted electrodes targeting the mPFC. Inter-train intervals (ITI) were varied systematically across five conditions (4s, 10s, 20s, 40s, 60s). Sham animals were connected to the stimulator but received no stimulation.

Calcium Imaging and Data Processing

In vivo imaging captured cellular fluorescence during and for 40 minutes post-TBS. Data were motion corrected, segmented, and $\Delta F/F$ traces extracted using CNMF-E. Neurons were classified as excited, inhibited, or unchanged based on z-scored fluorescence during stimulation and post-stimulation epochs.

Histology

Brains were perfused and sectioned for immunohistochemistry. Antibodies against GAD65, PV, and SST were used to assess GABAergic marker expression in the mPFC.

Statistical Analysis

Statistical analyses included Chi-square tests, two-way ANOVAs, and McNemar's tests, with Sidak corrections for multiple comparisons. Data was analyzed using MATLAB and GraphPad Prism.

Materials and methods

Subjects

The study utilized five female Long Evans rats, obtained from Charles River Laboratories. Upon arrival, rats (~150 g, approximately one-month-old) were housed in pairs within standard plastic cages (Allentown, NJ, USA) and acclimated for two weeks prior to surgery. Post-surgery, animals were individually housed to facilitate recovery. Rats were maintained under a 12-hour light/dark cycle (lights on at 6 a.m.), with experimental procedures conducted during the light phase. Food and water were available ad libitum. At the onset of recording experiments, rats weighed between 300–600 grams and were 3–5 months old. 26 rats included (5 per glutamatergic and GABAergic calcium imaging group, 16 rats for histology). 11 rats were excluded for electrolens misplacements (8 rats), and staining failure (3 rats).

Electrolens Fabrication

To deliver theta burst stimulation (TBS), electrodes were fabricated by attaching four 50 µm tungsten wires (California Fine Wire) with epoxy alongside an integrated ProView lens. Wires were spaced 100 µm apart beneath the lens edge. Optimal electrodes for effective calcium response were selected. A 75 µm stainless-steel wire (A-M Systems, Sequim, WA, USA) served as the ground, soldered to a stainless steel bone screw (Fine Science Tools).

Surgical Procedures

Stereotaxic surgery was performed under sterile conditions. Rats were anesthetized initially with 5% isoflurane and maintained at 1.9–2.5% throughout surgery, with body temperature regulated via a heating mat (VWR, Radnor, PA, USA). Atropine (0.05 mg/kg) reduced respiratory secretions; Dexamethasone (0.5 mg/kg) minimized inflammation; saline (1 mL, 0.9%) provided hydration; and Lidocaine (0.2 cc max) offered local analgesia. After incision and skull exposure, anchor and ground screws were inserted. A hole (1.2 mm diameter) was drilled at coordinates targeting the medial prefrontal cortex (mPFC; AP=+4.2 mm, ML=0.7 mm). Viral vectors (targeting either glutamatergic [CamKII-driven GCaMP] or GABAergic [mDlx-driven GCaMP] neurons) were infused (100 nL/min) at DV=2.8 mm and allowed to diffuse for 10 min post-infusion. An integrated ProView lens (1 mm diameter, 9 mm length) was implanted at DV=2.4 mm, sealed with Kwik-Sil (WPI), and secured using dental cement. Electrodes were connected to a TDT ZCA-EIB32 ZIF-Clip® Headstage-to-Electrode Interface Board. Post-surgical analgesics were administered as required. Procedures adhered strictly to NIH guidelines and were approved by the San Diego VA Medical Center IACUC (Protocol Number A12-021).

Data Processing and Analysis

Data processing and analysis were conducted using MATLAB v2023a. Cells were classified based on their normalized activity throughout the entire recording session. Normalization was performed using Z-score transformation, with the 5-minute period preceding the onset of TBS serving as the baseline for each cell. Cells were classified as 'excited', 'inhibited', or 'non-responsive' based on their activity during the TBS period compared to baseline activity. To reduce noise and ensure cleaner comparisons, average activity within 4-second time bins was used, resulting in 15 samples per minute of recording. Classification was carried out using the Wilcoxon rank-sum test in MATLAB, with a significance threshold of $p < 0.01$. Additionally, for analyses involving neuronal response stability (Figure 4), cells were further sorted based on their activity across the entire 40-minute post-stimulation period relative to baseline, allowing for evaluation of the consistency of neuronal identity over time.

To evaluate the relationship between neuronal activity during the TBS and post-TBS periods, a linear regression model was implemented in MATLAB, with activity during TBS as the independent variable (X) and post-TBS activity as the dependent variable (Y). The results included regression coefficients, 95% confidence intervals, R^2 values (goodness of fit), and Pearson's correlation coefficients, providing insights into the stability and consistency of neuronal responses across different stimulation intervals.

Theta Burst Stimulation (TBS) Protocol

TBS was administered via a Tucker-Davis Technologies IZ2H stimulator and passive ZIF-Clip® headstages. Electrical stimulation was comprised of 20 trains of 10 bursts, with each burst containing 3 biphasic, cathode-leading pulses (100 µA, 400 µs pulse width). Inter-train intervals (ITIs) ranged from 4 to 60 seconds, defined from the start of consecutive trains. Bursts and pulses were administered at 5 Hz and 50

Hz, respectively. The stimulation was facilitated via tungsten electrodes that were secured to the imaging lens.

Sham Experimental Condition

For the calcium imaging experiments, animals previously used in stimulation sessions were reconnected to the imaging and stimulation apparatus under identical conditions in the separate session, but no current was delivered. Data from these sessions were processed using the same analytical pipeline as the stimulation experiments to ensure methodological consistency. In the histological experiments, sham animals underwent identical surgical implantation of electrodes and were connected to the stimulation device without receiving any stimulation, thereby controlling for procedural and handling variables.

Histological Assessment

Tissue Preparation

At the conclusion of calcium imaging experiments, rats were deeply anesthetized and transcardially perfused with 0.9% saline followed by 4% paraformaldehyde (PFA) in phosphate-buffered saline (PBS). Extracted brains were post-fixed overnight at 4°C in 4% PFA, followed by cryoprotection in 30% sucrose solution in PBS until fully submerged. Coronal brain sections (40 µm thickness) were prepared using a cryostat (Leica CM1950, Leica Biosystems) and collected onto gelatin-coated slides. Sections were air-dried, rehydrated in PBS, and stored at 4°C until processing.

Verification of Viral Expression in Calcium Imaging Rats

To confirm successful viral delivery and expression in rats utilized for calcium imaging, brain sections were mounted onto slides, counterstained with DAPI (4′,6-diamidino-2-phenylindole), and coverslipped with antifade mounting medium (Fluoromount-G). Images were captured using confocal microscopy (Zeiss LSM 880, Zeiss Microscopy) and matched to the Paxinos and Watson rat brain atlas to verify accurate targeting of the medial prefrontal cortex.

Immunohistochemical Assessment of c-Fos and GAD-65

A separate cohort of rats (n = 4 per group) underwent TBS at ITIs of 4, 10, or 20 seconds or served as sham (electrode implantation and connection without stimulation), and were perfused 60 minutes post-stimulation. Sections underwent either double or triple immunofluorescence staining.

Double Staining (c-Fos and GAD-65):

One section per animal was incubated overnight at 4°C with primary antibodies purchased from Abcam:

- c-Fos: Anti-c-Fos monoclonal antibody [2H2], host: Mouse (Abcam, cat# ab208942, 1:1000 dilution)
- GAD-65: Anti-GAD-65 monoclonal antibody [EPR22952-70], host: Rabbit (Abcam, cat# EPR22952-70, 1:300 dilution)

Sections were subsequently incubated for 2 hours at room temperature with secondary antibodies from Thermo Fisher (1:500 dilution):

- Donkey anti-Mouse IgG (H+L), Alexa Fluor™ Plus 488 (Thermo Fisher, cat# A32766, green)
- Donkey anti-Rabbit IgG (H+L), Alexa Fluor™ 568 (Thermo Fisher, cat# A10042, red)

Quantification of immunoreactivity intensity for double staining was conducted using FIJI (ImageJ). Regions of interest (ROIs; 500 µm spanning around the stimulation electrode) were analyzed and data averaged per animal for statistical comparisons.

Triple Staining (PV, SST, and GAD-65):

Another section per animal was incubated overnight at 4°C with primary antibodies purchased from Abcam:

- Parvalbumin (PV): Polyclonal antibody, host: Chicken (Abcam, cat# PA5-143579, 1:300 dilution)
- Somatostatin (SST): Monoclonal antibody [7G5], host: Mouse (Abcam, cat# MA5-17182, 1:300 dilution)
- GAD-65: Anti-GAD-65 monoclonal antibody [EPR22952-70], host: Rabbit (Abcam, cat# EPR22952-70, 1:300 dilution)

Sections were subsequently incubated for 2 hours at room temperature with secondary antibodies from Thermo Fisher (1:500 dilution):

- Donkey anti-Chicken IgY (H+L), Alexa Fluor™ 647 (Thermo Fisher, cat# A78952, far red, PV)
- Donkey anti-Mouse IgG (H+L), Alexa Fluor™ Plus 488 (Thermo Fisher, cat# A32766, green, SST)
- Donkey anti-Rabbit IgG (H+L), Alexa Fluor™ 568 (Thermo Fisher, cat# A10042, red, GAD-65)

Confocal microscopy (Zeiss LSM 880) was used for high-resolution image acquisition. For quantitative analyses, Imaris software (Oxford Instruments) was employed to perform three-dimensional cellular reconstruction, quantify immunoreactivity intensity within individual cells, and assess colocalization of

GAD-65 with PV and SST interneurons using Mander's coefficients only in ROI-1 corresponding 500 µm spanning around the stimulation electrode.

Statistical Analysis

Statistical analyses were conducted using IBM SPSS Statistics (Version 29) and GraphPad Prism software for data visualization. To evaluate the effects of theta burst stimulation (TBS) across different inter-train intervals (ITIs), two-way ANOVA models were applied, with stimulation condition ITI duration or sham as group factor and 8 discrete of 5min for 40 min post time bins as time bin factor, to assess interactions between these variables. One-way ANOVAs were used for analyses of cellular activity specifically within the stimulation period across different ITIs. Post-hoc comparisons following ANOVA analyses were corrected using Sidak's correction for multiple comparisons, with statistical significance set at $p<0.05$. Data are presented as mean ± SEM. Linear regression analysis was used to assess correlations between neuronal activity during and post-TBS periods. Post-TBS activity served as the dependent variable (Y), with during-TBS activity as the independent variable (X). Regression coefficients, R^2 values (goodness of fit), 95% confidence intervals, and Pearson's correlation coefficients were reported. For categorical comparisons (cell proportions and identity stability analyses), Chi-square and McNemar's tests were employed, respectively. Prior to these tests, cell category data were transformed into binary form (e.g., excited vs. not-excited; inhibited vs. not-inhibited) to accurately reflect the proportions and cell counts. Specifically, McNemar's test was utilized to determine changes in cell identity classifications between TBS and post-TBS periods. All statistical tests were two-tailed, and significance was established at a threshold of $p<0.05$.

Acknowledgments

We would like to thank Miranda Koloski for her assistance for data collection. This material is the result of work supported with resources and the use of facilities at the VA San Diego Medical Center and the Center of Excellence for Stress and Mental Health. The contents of this manuscript do not represent the views of the U.S. Department of Veteran Affairs or the United States Government. This study was supported by the following grants. Dhakshin Ramanathan, Burroughs Wellcome Fund (https://dx.doi.org/10.13039/100000861), Award ID: 1015644. Dhakshin Ramanathan, National Institute of Mental Health (https://dx.doi.org/10.13039/100000025), Award ID: R01MH123650. Jyoti Mishra , Hope for Depression Research Foundation. Grant ID: 30063773. We also acknowledge the UCSD School of Medicine Microscopy Core Grant P30 NS047101.

Author contributions

Conceptualization, MS, DR.; technical development, MS , MN and Jonathan M. investigation, MS.; analysis, MS and MN, SJ, JR; resources and funding acquisition, DR, Jyoti M.; writing original draft MS, DR, MN and SJ; writing reviewing & editing, MS, DR, MN, JR, Jonathan M and Jyoti M.

Declaration of Interest

The author declares no conflicts of interest related to this study. The views expressed in this article are those of the authors and do not necessarily reflect the position or policy of the VA or the NIH. The funders had no role in the design of the study, data analysis, or decision to publish. The authors have no relevant biomedical conflicts of interest to disclose.

References

1. Chung SW, Hoy KE, Fitzgerald PB. Theta-Burst Stimulation: A New Form of Tms Treatment for Depression? Depression and Anxiety. 2015;32(3):182–92.

2. Huang YZ, Edwards MJ, Rounis E, Bhatia KP, Rothwell JC. Theta Burst Stimulation of the Human Motor Cortex. Neuron. 2005 Jan;45(2):201–6.

3. Larson J, Munkácsy E. Theta-burst LTP. Brain Research. 2015 Sep;1621:38–50.

4. Barker AT, Jalinous R, Freeston IL. Non-invasive magnetic stimulation of human motor cortex. The Lancet. 1985;325(8437):1106–7.

5. Hamlin D, Garman J. A Brief History of Transcranial Magnetic Stimulation. AJP Residents' Journal. 2023 Mar 1;18(3):8–10.

6. Jannati A, Oberman LM, Rotenberg A, Pascual-Leone A. Assessing the mechanisms of brain plasticity by transcranial magnetic stimulation. Neuropsychopharmacol. 2023 Jan;48(1):191–208.

7. Larson J, Wong D, Lynch G. Patterned stimulation at the theta frequency is optimal for the induction of hippocampal long-term potentiation. Brain Research. 1986 Mar;368(2):347–50.

8. Li C, Huang Y, Bai Y, Tsai S, Su T, Cheng C. Critical role of glutamatergic and GABAergic neurotransmission in the central mechanisms of theta‐burst stimulation. Hum Brain Mapp. 2019 Jan 1;40(6):2001–9.

9. Benali A, Trippe J, Weiler E, Mix A, Petrasch-Parwez E, Girzalsky W, et al. Theta-Burst Transcranial Magnetic Stimulation Alters Cortical Inhibition. J Neurosci. 2011 Jan 26;31(4):1193–203.

10. Huang YZ, Lu MK, Antal A, Classen J, Nitsche M, Ziemann U, et al. Plasticity induced by non-invasive transcranial brain stimulation: A position paper. Clinical Neurophysiology. 2017 Nov;128(11):2318–29.

11. Huang YZ, Rothwell JC, Chen RS, Lu CS, Chuang WL. The theoretical model of theta burst form of repetitive transcranial magnetic stimulation. Clinical Neurophysiology. 2011 May;122(5):1011–8.

12. Blumberger DM, Vila-Rodriguez F, Thorpe KE, Feffer K, Noda Y, Giacobbe P, et al. Effectiveness of theta burst versus high-frequency repetitive transcranial magnetic stimulation in patients with depression (THREE-D): a randomised non-inferiority trial. The Lancet. 2018 Apr 28;391(10131):1683–92.

13. Chung SW, Hoy KE, Fitzgerald PB. Theta-Burst Stimulation: A New Form of Tms Treatment for Depression? Depression and Anxiety. 2015;32(3):182–92.

14. Chung SW, Hoy KE, Fitzgerald PB. Theta-Burst Stimulation: A New Form of Tms Treatment for Depression? Depression and Anxiety. 2015;32(3):182–92.

15. Chung SW, Hill AT, Rogasch NC, Hoy KE, Fitzgerald PB. Use of theta-burst stimulation in changing excitability of motor cortex: A systematic review and meta-analysis. Neuroscience & Biobehavioral Reviews. 2016 Apr 1;63:43–64.

16. Di Lazzaro V, Ziemann U. The contribution of transcranial magnetic stimulation in the functional evaluation of microcircuits in human motor cortex. Front Neural Circuits [Internet].

2013 Feb 13 [cited 2025 Mar 30];7. Available from: https://www.frontiersin.org/journals/neural-circuits/articles/10.3389/fncir.2013.00018/full

17. Huang YZ, Chen RS, Rothwell JC, Wen HY. The after-effect of human theta burst stimulation is NMDA receptor dependent. Clinical Neurophysiology. 2007 May;118(5):1028–32.

18. Jin J, Wang X, Wang H, Li Y, Liu Z, Yin T. Train duration and inter-train interval determine the direction and intensity of high-frequency rTMS after-effects. Front Neurosci. 2023 Jul 5;17:1157080.

19. Hinder MR, Goss EL, Fujiyama H, Canty AJ, Garry MI, Rodger J, et al. Inter- and Intra-individual Variability Following Intermittent Theta Burst Stimulation: Implications for Rehabilitation and Recovery. Brain Stimulation. 2014 May;7(3):365–71.

20. Cormier RJ, Greenwood AC, Connor JA. Bidirectional Synaptic Plasticity Correlated With the Magnitude of Dendritic Calcium Transients Above a Threshold. Journal of Neurophysiology. 2001 Jan;85(1):399–406.

21. Nanou E, Catterall WA. Calcium Channels, Synaptic Plasticity, and Neuropsychiatric Disease. Neuron. 2018 May 2;98(3):466–81.

22. Kotak VC, Mirallave A, Mowery TM, Sanes DH. GABAergic inhibition gates excitatory LTP in perirhinal cortex. Hippocampus. 2017;27(12):1217–23.

23. Jappy D, Valiullina F, Draguhn A, Rozov A. GABABR-Dependent Long-Term Depression at Hippocampal Synapses between CB1-Positive Interneurons and CA1 Pyramidal Cells. Front Cell Neurosci [Internet]. 2016 Jan 28 [cited 2025 Apr 10];10. Available from: http://journal.frontiersin.org/Article/10.3389/fncel.2016.00004/abstract

24. Stäubli U, Scafidi J, Chun D. GABAB Receptor Antagonism: Facilitatory Effects on Memory Parallel Those on LTP Induced by TBS but Not HFS. J Neurosci. 1999 Jun 1;19(11):4609–15.

25. Kaster TS, Downar J, Vila-Rodriguez F, Thorpe KE, Feffer K, Noda Y, et al. Trajectories of response to dorsolateral prefrontal rTMS in major depression: a THREE-D study. American Journal of Psychiatry. 2019;176(5):367–75.

26. Currant T. Role of ion ftux in the control of c-fos expression. 1986;

27. Patel AB, de Graaf RA, Martin DL, Battaglioli G, Behar KL. Evidence that GAD65 mediates increased GABA synthesis during intense neuronal activity in vivo. Journal of neurochemistry. 2006;97(2):385–96.

28. Tremblay R, Lee S, Rudy B. GABAergic Interneurons in the Neocortex: From Cellular Properties to Circuits. Neuron. 2016 Jul;91(2):260–92.

29. Urban-Ciecko J, Barth AL. Somatostatin-expressing neurons in cortical networks. Nat Rev Neurosci. 2016 Jul;17(7):401–9.

30. Nishiyama M, Togashi K, Aihara T, Hong K. GABAergic activities control spike timing- and frequency-dependent long-term depression at hippocampal excitatory synapses. Front Synaptic Neurosci [Internet]. 2010 Jun 23 [cited 2025 Mar 31];2. Available from: https://www.frontiersin.org/journals/synaptic-neuroscience/articles/10.3389/fnsyn.2010.00022/full

31. Szydlowski SN, Pollak Dorocic I, Planert H, Carlén M, Meletis K, Silberberg G. Target Selectivity of Feedforward Inhibition by Striatal Fast-Spiking Interneurons. J Neurosci. 2013 Jan 23;33(4):1678–83.

32. Hijazi S, Smit AB, van Kesteren RE. Fast-spiking parvalbumin-positive interneurons in brain physiology and Alzheimer's disease. Mol Psychiatry. 2023 Dec;28(12):4954–67.

33. Zucker RS, Regehr WG. Short-term synaptic plasticity. Annual review of physiology. 2002;64(1):355–405.

34. Fioravante D, Regehr WG. Short-term forms of presynaptic plasticity. Current opinion in neurobiology. 2011;21(2):269–74.

35. Murakami T, Müller-Dahlhaus F, Lu M, Ziemann U. Homeostatic metaplasticity of corticospinal excitatory and intracortical inhibitory neural circuits in human motor cortex. The Journal of physiology. 2012;590(22):5765–81.

36. Huang YZ, Rothwell JC, Chen RS, Lu CS, Chuang WL. The theoretical model of theta burst form of repetitive transcranial magnetic stimulation. Clinical Neurophysiology. 2011;122(5):1011–8.

37. Miles R, Le Duigou C, Simonnet J, Telenczuk M, Fricker D. Recurrent synapses and circuits in the CA3 region of the hippocampus: an associative network. Front Cell Neurosci [Internet]. 2014 Jan 8 [cited 2025 Apr 16];7. Available from: https://www.frontiersin.orghttps://www.frontiersin.org/journals/cellular-neuroscience/articles/10.3389/fncel.2013.00262/full

38. Kullmann DM, Lamsa KP. Long-term synaptic plasticity in hippocampal interneurons. Nat Rev Neurosci. 2007 Sep;8(9):687–99.

39. Lenz M, Vlachos A. Releasing the cortical brake by non-invasive electromagnetic stimulation? rTMS induces LTD of GABAergic neurotransmission. Frontiers in Neural Circuits. 2016;10:96.

40. Lenz M, Galanis C, Müller-Dahlhaus F, Opitz A, Wierenga CJ, Szabó G, et al. Repetitive magnetic stimulation induces plasticity of inhibitory synapses. Nature communications. 2016;7(1):10020.

41. Le Duigou C, Kullmann DM. Group I mGluR Agonist-Evoked Long-Term Potentiation in Hippocampal Oriens Interneurons. J Neurosci. 2011 Apr 13;31(15):5777–81.

42. Grover LM, Yan C. Blockade of $GABA_A$ Receptors Facilitates Induction of NMDA Receptor-Independent Long-Term Potentiation. Journal of Neurophysiology. 1999 Jun 1;81(6):2814–22.

43. Romero MC, Merken L, Janssen P, Davare M. Neural effects of continuous theta-burst stimulation in macaque parietal neurons. Elife. 2022;11:e65536.

44. Abraham WC, Bear MF. Metaplasticity: the plasticity of synaptic plasticity. Trends in neurosciences. 1996;19(4):126–30.

45. Todd G, Flavel SC, Ridding MC. Priming theta-burst repetitive transcranial magnetic stimulation with low-and high-frequency stimulation. Experimental Brain Research. 2009;195:307–15.

46. Kuo HI, Bikson M, Datta A, Minhas P, Paulus W, Kuo MF, et al. Comparing cortical plasticity induced by conventional and high-definition 4× 1 ring tDCS: a neurophysiological study. Brain stimulation. 2013;6(4):644–8.

47. Gentner R, Wankerl K, Reinsberger C, Zeller D, Classen J. Depression of human corticospinal excitability induced by magnetic theta-burst stimulation: evidence of rapid polarity-reversing metaplasticity. Cerebral cortex. 2008;18(9):2046–53.

48. Gamboa OL, Antal A, Moliadze V, Paulus W. Simply longer is not better: reversal of theta burst after-effect with prolonged stimulation. Experimental brain research. 2010;204(2):181–7.

49. Gamboa OL, Antal A, Laczo B, Moliadze V, Nitsche MA, Paulus W. Impact of repetitive theta burst stimulation on motor cortex excitability. Brain stimulation. 2011;4(3):145–51.

50. Galarreta M, Hestrin S. A network of fast-spiking cells in the neocortex connected by electrical synapses. Nature. 1999;402(6757):72–5.

51. Hu H, Gan J, Jonas P. Fast-spiking, parvalbumin+ GABAergic interneurons: From cellular design to microcircuit function. Science. 2014;345(6196):1255263.

52. Moretti J, Terstege DJ, Poh EZ, Epp JR, Rodger J. Low intensity repetitive transcranial magnetic stimulation modulates brain-wide functional connectivity to promote anti-correlated c-Fos expression. Scientific Reports. 2022;12(1):20571.

53. Funke K, Benali A. Modulation of cortical inhibition by rTMS–findings obtained from animal models. The Journal of physiology. 2011;589(18):4423–35.

54. Feldman DE. The Spike-Timing Dependence of Plasticity. Neuron. 2012 Aug 23;75(4):556–71.

55. Larson J, Lynch G. Theta pattern stimulation and the induction of LTP: the sequence in which synapses are stimulated determines the degree to which they potentiate. Brain Research. 1989 Jun;489(1):49–58.

56. Nettekoven C, Volz LJ, Leimbach M, Pool EM, Rehme AK, Eickhoff SB, et al. Inter-individual variability in cortical excitability and motor network connectivity following multiple blocks of rTMS. Neuroimage. 2015;118:209–18.

57. Leodori G, Fabbrini A, De Bartolo MI, Costanzo M, Asci F, Palma V, et al. Cortical mechanisms underlying variability in intermittent theta-burst stimulation-induced plasticity: A TMS-EEG study. Clinical Neurophysiology. 2021 Oct;132(10):2519–31.

58. Dhami P, Moreno S, Croarkin PE, Blumberger DM, Daskalakis ZJ, Farzan F. Baseline markers of cortical excitation and inhibition predict response to theta burst stimulation treatment for youth depression. Scientific reports. 2023;13(1):19115.